S+IF

NASA Technical Memorandum 89453

Adaptive Control and Noise Suppression by a Variable-Gain Gradient Algorithm

S.J. Merhav and R.S. Mehta

June 1987

National Aeronautics and Space Administration

NASA Technical Memorandum 89453

Adaptive Control and Noise Suppression by a Variable-Gain Gradient Algorithm

S.J. Merhav, Israel Institute of Technology, Haifa, Israel
R.S. Mehta, Ames Research Center, Moffett Field, California

June 1987

National Aeronautics and
Space Administration

Ames Research Center
Moffett Field, California 94035

List of Symbols

d	desired filter output
dt	integration time step in seconds in computer simulation
D, D'	characteristic polynomial in noise suppression schemes
e	filter error
f	factor used in calculating adaptation gain
g	delay operator
G	adaptive controller
G_c	copy of adaptive controller
G_i	compensator including integral control
i	subscript index of filter weight
j	iteration number
M	open loop reference model
M_w	misadjustment of filter weights
n	output referred noise — without noise suppression
n_s	output referred noise — with noise suppression
N	number of filter weights
N'	subset of N, used in variable gain scheme
P	the unknown plant
$r(\cdot)$	relative degree of
$rms(\cdot)$	root mean square of
R	correlation matrix of input to FIR
$Re(\cdot)$	real part of
s	differential operator
$tr(\cdot)$	trace of
ΔT	discretization time in FIR
T_f	length of FIR
T_m	closed loop reference model
T_u	actual closed loop system
u	input control signal
v	measurement noise
$var(\cdot)$	variance of
w	process noise
w_i	i-th filter weight
x	filter input
y	filter output, output of adaptive controller
z	plant output
z_m	measured plant output
z_r	output of closed loop reference model
α	measure of effectiveness of noise suppression
ϵ	system error used for noise suppresion
ε	measure of filter error used in variable gain scheme
ε_s	saturation of ε in variable gain scheme
ε_t	threshold in variable gain scheme
ζ	damping factor
λ	eigenvalue

μ	gain of adaptive algorithm
σ_A	standard deviation of signal A
τ	adaptation time constant in number of iterations
τ_s	settling time of adaptation algorithm in seconds
ω	natural frequency
ω_A	cut-off frequency of system A

Acronyms

FIR	Finite Impulse Response
IIR	Infinite Impulse Response
LMS	Least Mean Squared
PSD	Power Spectral Density
RLS	Recursive Least Squares

SUMMARY

An adaptive control system based on normalized variable-gain LMS filters is investigated. The finite impulse response of the nonparametric controller is adaptively estimated using a given reference model. Specifically, the following issues are addressed: The stability of the closed loop system is analyzed and heuristically established. Next, the adaptation process is studied for piecewise constant plant parameters. It is shown that by introducing a variable-gain in the gradient algorithm, a substantial reduction in the LMS adaptation rate can be achieved. Finally, process noise at the plant output generally causes a biased estimate of the controller. By introducing a noise suppression scheme, this bias can be substantially reduced and the response of the adapted system becomes very close to that of the reference model. Extensive computer simulations validate these and demonstrate assertions that the system can rapidly adapt to random jumps in plant parameters.

1 INTRODUCTION

One of the primary goals in current control-systems research is the achievement of robustness to plant-parameter uncertainties and variations. The principal approaches are robust and adaptive control. In recent surveys and texts [1], [2], [3] , a nominal parametric plant model, describable by a finite state space equation, is assumed in the computation of the controller. The convergence and stability of the closed-loop system depends on the realism of this model, specifically on the correctness of the order and relative degree of its input-output transfer functions [4].

The difficulties in assuring the realism of the plant model have thus far prevented the analytical accomplishments in adaptive control theory from translating into design methods for practical processes. This paper explores an alternative approach to adaptive control design through implementation of a "nonparametric" finite impulse response (FIR) realization of the controller. At the expense of excluding nonminimum phase plants and assuming that, if necessary, stability can be provided by an inner feedback loop, it is demonstrated that the nonparametric FIR approach can provide a highly robust controller.

The advent of adaptive filters [5], [6], and their successful applications to identification and noise cancellation [7], and more recently to interference suppression in control systems [8], [9], has spurred interest in applying self-adjusting finite impulse response (FIR) filters as a building block in model reference adaptive control (MRAC) systems [10], [11], [12]. In this approach, the realization of the controller is not subject to the stringent conditions required in the parametric realizations. The large number of weights used in the FIR provides great flexibility and makes the controller insensitive to uncertainties in the order and the relative degree of the plant model.

In these previous studies, the controller is directly identified by means of an open-loop reference model and it converges to a filtered inverse of the plant. This implies adaptive pole-zero cancellation. Consequently this method is restricted to stable or stabilized minimum-phase plants. In the present paper, which is based on [10] and [11], the same restriction holds. A major problem in the integration of adaptive FIR filters into closed-loop control systems is the possible violation of the linearity of the error equation, which is a necessary condition for the global and uniform convergence of the adaptive algorithm. For this and

other reasons, this approach in earlier work, such as [12], has resulted in open-loop control configurations only. In [10], the integration of FIR adaptive filters in closed-loop MRAC systems is studied in detail and in [11], a heuristic argument for the global convergence and stability of the closed-loop system is given.

The penalty for the robustness of adaptive FIR realizations such as LMS or recursive least squares (RLS) is a relatively slow adaptation to plant parameter variations. The reason for this slow adaptation in LMS or RLS realizations, [13], is that rapid adaptation involves a large weight noise which results in deteriorated system response. This conflict cannot be resolved in a conventional LMS or RLS realization in which the adaptation gain or the forgetting factor, respectively, is constant. In this paper we present a "variable gain" algorithm which resolves this conflict to a great extent. As a result, substantially faster adaptation rates can be achieved.

Another issue is that process noise causes bias in the FIR estimate of the controller. This bias can cause substantial distortion of the closed-loop response [10]. In this paper we present a noise suppression scheme which substantially reduces controller bias. This scheme permits the independent design of system response and noise suppression without resorting to prefiltering methods which involve an undesirable increase in system order.

Throughout this paper, the conventional LMS algorithm is the basis of analysis and computer simulation. Recent results in fast recursive least squares (FRLS) [13], [14] indicate that a further increase in adaptation rate and precision in parameter tracking is possible. It is expected that if FRLS is implemented with an adaptive forgetting factor, analogous to the variable-gain LMS presented in this paper, a still further increase in adaptation rate can be achieved.

2 MODEL REFERENCE ADAPTIVE CONTROL USING THE LEAST-MEAN-SQUARE FILTER

In this section, the basic control system, in which an LMS filter is used as the controller in a model reference adaptive control scheme, is reviewed. An analysis of its properties, in particular the effect of noise, leads to the improvements in the control system addressed in following sections.

2.1 The Adaptive Finite Impulse Response Model

It is well known that the continuous, i.e., infinite, impulse response (IIR) of a system can be represented by a finite set of parameters by truncating and discretizing the response. The fidelity of the FIR depends on the fineness of discretization ΔT and the length of time T_f before truncation. The FIR is expressed in the form of a moving average model as shown in (fig. 1). The input to the model is sampled. Then the present and past $N-1$ values are stored in a tapped-delay line. These values are then weighted and summed to form the model output y_j. The symbol g represents an operator which produces a given length of delay. The model contains two parameters — the number of weights N and the length of

the delay g. Equation 1 describes this model at time j :

$$y_j = \sum_{i=0}^{N-1} w_{i_j} g^i x_j = \underline{w}_j^T \underline{x}_j \tag{1}$$

where

$$g^i x_j \equiv x_{j-i} \tag{2}$$

$$\underline{w}_j \triangleq \left[w_{0_j}\ w_{1_j}\ \cdots\ w_{(N-1)_j} \right]^T$$
$$\underline{x}_j \triangleq \left[x_j\ x_{j-1}\ \cdots\ x_{j-(N-1)} \right]^T$$

The weights w_i also have the subscript j, to indicate their time-varying character. The model can be made adaptive by including an algorithm which adjusts the weights so that y_j matches a desired signal d_j as shown in figure 1. The adaptation is implemented by a gradient algorithm. The combination of the moving average model and a gradient algorithm is known as the LMS filter [7].

The filter error equation, where d_j is the desired output, is

$$e_j = d_j - y_j = d_j - \underline{w}_j^T \underline{x}_j \tag{3}$$

The weights are adjusted by minimizing the square of the filter error e_j^2 as follows :

$$\underline{w}_{j+1} = \underline{w}_j + \Delta \underline{w}_j \tag{4}$$

$$\Delta \underline{w}_j = -\mu \left. \frac{\partial e_j^2}{\partial \underline{w}} \right|_{\underline{w}=\underline{w}_j} = -2\mu e_j \left. \frac{\partial e_j}{\partial \underline{w}} \right|_{\underline{w}=\underline{w}_j} \tag{5}$$

The gradient of the error can be derived from equation (3)

$$\left. \frac{\partial e_j}{\partial \underline{w}} \right|_{\underline{w}=\underline{w}_j} = -\underline{x}_j \tag{6}$$

leading to a weight-update equation

$$\Delta \underline{w}_j = 2\mu e_j \underline{x}_j \tag{7}$$

where μ is a gain factor that is chosen in consideration of the stability of the gradient algorithm. In the traditional LMS filter, μ is a constant. The properties of the LMS filter have been studied extensively [3],[5]. Some of them are summarized in section 2.4. This paper introduces an algorithm that allows a variable μ. One important aspect of the LMS filter is the assumption inherent in equation (6), which is that neither the desired signal d nor the input to the filter x are functions of the filter weights w_i.

2.2 The Control System Configuration

Although the LMS filter itself is a discrete system, the entire control system will be analyzed as a continuous system. The fundamental building block of the model reference adaptive

control (MRAC) in this paper is shown in figure 2 where $s \triangleq \frac{d}{dt}$ is the differential operator, $P(s)$ is the unknown plant, $M(s)$ is a reference model, and $G(s)$ is the controller which adapts such that $P(s)G(s) \rightarrow M(s)$ to minimize the error e. The input signal is u and the plant output is z. The controller $G(s)$ and its associated adaptation algorithm are modeled as an LMS filter. It is clear from figure 2 that the signals d and z are independent of w_i, which are the weights in G, and that e is linear in w_i satisfying the assumptions of the LMS filter.

To obtain open-loop control, an exact copy of G, G_c, is placed before P (fig. 3). The controller G_c now provides open-loop control of P; once G has properly adapted, the input-output relation (from u to z) is determined by $GP = M$. It is apparent from figure 3 that both d and z are now dependent on w_i. This essentially violates one of the basic assumptions of the LMS filter. The issue will be addressed in the next section.

In figure 4, closed-loop control is achieved by feeding back the signal y. Controllers G and G_c now forms a controller with unity feedback. The signals w and v represent process noise and measurement noise, respectively. The block T_m represents the desired closed-loop response of the system; its output is z_r.

The additional operator G_i provides integral control. It is needed to satisfy the following two requirements:

1. $\lim_{s \rightarrow 0} T_m(s) = 1$
2. $\lim_{s \rightarrow 0} M(s) =$ constant

The first requirement is a standard specification for closed-loop control. The second is to assure the realizability of G. Requirement 2 specifies that M, and by implication G, should not incorporate a free integrator. If that were the case, its infinite impulse response could not have been represented by a finite impulse response. With $GP = M$, the closed-loop reference model T_m is :

$$T_m = \frac{MG_i}{1 + MG_i} \tag{8}$$

which satisfies requirements 1 and 2.

2.3 Convergence

The signals d and z in figure 4 are dependent on the filter weights w_i and therefore the convergence of the LMS filter is not assured. Because of this, it was initially reasoned [10],[11] that the system should be started in the adaptive-element mode (fig. 2) and then switched to the closed-loop control configuration (fig. 4) after the controller G had converged. However, the system can converge completely in the closed-loop configuration. A heuristic argument for this convergence, which is given in [11], is summarized here.

For the following discussion, we will assume that there is no noise and that G_i is given by

$$G_i = \frac{1}{s} \tag{9}$$

The filter error at the j-th iteration is

$$e_j = \frac{(M - GP)G}{s + GP} u_j \tag{10}$$

and the error gradient is

$$\left(\frac{\partial e}{\partial w_i}\right)_j = \frac{Ms - GP(2s + GP)}{(s + GP)^2} g^i u_j \triangleq -D_T g^i u_j \tag{11}$$

which can also be written as

$$\left(\frac{\partial e}{\partial w_i}\right)_j = \underbrace{-g^i z_j}_{\triangleq -D_I g^i u_j} + \frac{s}{G(s + GP)} g^i e_j \tag{12}$$

Comparing equation (12) with equation (6), which is the required expression for the error gradient for the LMS filter, we note that $g^i z_j$ represents $\underline{x}_j$ and that the difference lies in the second term in equation (12). It is not possible to compute the second term. Therefore, only the first term is used in the system implementation. The theoretical and implemented error-gradients are indicated by the use D_T and D_I, respectively.

It is obvious that when the filter has converged correctly and the error e_j is small, D_I will provide approximately the correct value $(-g^i z_j)$ for the error gradient. However, the question is whether $e_j \to 0$ as $j \to \infty$. In [11] it was shown that for a specific example, D_I was close to D_T even with large errors in the filter weights, as at the start of adaptation. This was done by comparing the Bode phase and magnitude responses of D_T and D_I. The analysis indicated that the contribution of the second term in equation (12) was small and that the implemented error-gradient D_I was sufficiently accurate for the convergence of the filter. This analysis has been confirmed by many computer runs using different plants and reference models, all of which have converged.

2.4 Parameter Choices and Tradeoffs

In the design of the control system shown in figure 4, it is necessary to choose the reference model M and the LMS filter parameters N, ΔT, and μ.

2.4.1 Reference Model

The reference model M is selected in accordance with standard control-system-design practices subject to the condition that $r(M) \geq r(P)$, where $r(\cdot)$ stands for the relative degree. For example, if G_i in equation (8) is chosen as $G_i = 1/s$, then

$$T_m = \frac{M}{s + M} \tag{13}$$

and $r(T_m) = r(M) + 1$. However, if it is desired that $r(T_m) = r(M)$, then a valid form for G_i is

$$G_i = \frac{a_1(s + a_0)}{s} \tag{14}$$

resulting in

$$T_m = \frac{a_1(s+a_0)M}{s+a_1(s+a_0)M} \tag{15}$$

Generally, T_m is specified; M and G_i are computed as demonstrated in section 3.

2.4.2 Filter Parameters

The adaptation process adjusts G so that $GP \rightarrow M$. Therefore, ideally $G = M/P$. This means that the characteristic equation of G includes the poles of M and the zeros of P.

In the discussion in section 2.1, we noted that the fidelity of the FIR depends on its length T_f and the time increment ΔT. To ensure a sufficiently small truncation error, the following design rule will be adopted: let $Re(\lambda_{min})$ be the real part of the smallest eigenvalue of $M(s)$, then choose T_f such that

$$T_f \geq \frac{4}{Re(\lambda_{min})} \tag{16}$$

This ensures a truncation error of less than 2% [10]. If the bandwidth of the filter input signal z is ω, the sampling theorem would require the following condition:

$$\Delta T \leq \frac{2\pi}{2\omega} = \frac{\pi}{\omega} \tag{17}$$

However, in accordance with control-system-design practice for stability and robustness, frequency components up to 10 times the open loop cutoff frequency ω_M should be reproduced. Since $GP \cong M$, a conservative requirement is that G should reproduce all frequency components up to $10\omega_M$. This leads to

$$\Delta T \leq \frac{2\pi}{2(10\omega_M)} = \frac{\pi}{10\omega_M} \tag{18}$$

In general, equation (18) is more limiting than equation (17). Once the filter length T_f and tap spacing ΔT have been chosen, the number of weights is given by

$$N = \frac{T_f}{\Delta T} + 1 \tag{19}$$

So, the number of weights in the FIR is determined by the desired degree of fidelity of the FIR to the ideal IIR. The use of fewer parameters than those required by equations (16) through (19) will provide reduced, but perhaps still acceptable, performance. In principle, fewer parameters can be used without sacrificing performance by using nonuniform tap spacing [10].

The gain factor μ is chosen to assure the stability of the adaptation process. Define R_j as the correlation matrix of the input to the FIR:

$$R_j \triangleq \underline{x}_j \underline{x}_j^T \tag{20}$$

where $\underline{x}_j$ is the vector of the signals at the delay-line taps, (fig. 1). The matrix R_j is real, symmetric and non-negative definite. It can be shown [5] that to ensure stable convergence, a sufficient condition is

$$0 < \mu < \frac{1}{\lambda_{max}} \tag{21}$$

where λ_{max} is the largest eigenvalue of R_j. Since λ_{max} is difficult to calculate, equation (21) is replaced by

$$0 < \mu < \frac{1}{tr(R_j)} \tag{22}$$

where $tr(R_j)$ is the trace of R_j. Since $tr(R_j) \geq \lambda_{max}$, equation (22) is more conservative than equation (21). In practive, μ is determined by

$$\mu_j = \frac{1}{f\, tr(R_j)} \quad ; \quad f > 1 \tag{23}$$

The factor f is chosen by the designer. It can be shown [5], that the average exponential-convergence time constant in terms of the number of iterations is given by

$$\tau = \frac{fN}{4} \tag{24}$$

An additional factor which is involved in the choice of μ is the misadjustment factor M_w, which is defined as the excess parameter noise $\Delta\underline{w}_m$ in $\underline{w}$ over the noise in the asymptotic Wiener solution [5]. It is given by

$$M_w = \frac{1}{f} \tag{25}$$

Thus the choice of f involves a fundamental conflict. A small f provides fast convergence but results in large parameter noise; conversely, a large f provides accurate convergence (low parameter noise) but takes longer to converge.

It should be noted that there exists a direct relation between the response time of the reference model M and the speed of convergence of the controller G. The convergence time, in seconds, of G can be determined from equation (24) by

$$\tau_s = (4\tau)\Delta T = fN\Delta T \tag{26}$$

Substituting equation (19) into equation (26) gives

$$\tau_s = f\left(\frac{T_f}{\Delta T} + 1\right)\Delta T \approx fT_f \tag{27}$$

Since the smallest eigenvalue of M determines T_f, (eq. (16)), the faster M is, the smaller the resulting value of τ_s. Thus, the choice of M is instrumental in the speed of adaptation of G.

2.5 Effect of Additive Noise

Additive noise, whether process noise or measurement noise, produces errors in the estimation process and biases the filter weights. These effects are easily seen by an examination of the adaptation algorithm equations. With regard to the effects on the weights of the

controller, process and measurement noise can be grouped together [10]. From figure 4, the input to the LMS filter is z_m.

$$z_{m_j} = z_j + n_j \tag{28}$$

where n_j represents the noise in the plant output caused by both w_j and v_j. The weight update produced by equation (7) is

$$\Delta \underline{w}_j = \underline{w}_{j+1} - \underline{w}_j = 2\mu e_j \underline{z}_{m_j} \tag{29}$$

where

$$\underline{z}_{m_j} \triangleq \left[z_{m_j} \; z_{m_{j-1}} \; \cdots \; z_{m_{j-(N-1)}} \right]^T$$

Since the filter error is

$$e_j = d_j - \underline{z}_{m_j}^T \underline{w}_j \tag{30}$$

$$\Delta \underline{w}_j = 2\mu d_j \underline{z}_{m_j} - 2\mu \underline{z}_{m_j} \underline{z}_{m_j}^T \underline{w}_j \tag{31}$$

As the system converges, $\Delta \underline{w}_j \to 0$, we obtain

$$0 = 2\mu E\left[d_j \underline{z}_{m_j}\right] - 2\mu E\left[\underline{z}_{m_j} \underline{z}_{m_j}^T \underline{w}^\circ\right] \tag{32}$$

If μ is small, the weights converge to a constant vector $\underline{w}^\circ$ given by

$$\underline{w}^\circ = E\left[\underline{z}_{m_j} \underline{z}_{m_j}^T\right]^{-1} E\left[d_j \underline{z}_{m_j}\right] \tag{33}$$

Assuming that n is uncorrelated with z and d

$$\underline{w}^\circ = E\left[\underline{z}_j \underline{z}_j^T + \underline{n}_j \underline{n}_j^T\right]^{-1} E\left[d_j \underline{z}_j\right] \tag{34}$$

If there were no noise, the weights would settle to the Wiener solution $\underline{w}^*$

$$\underline{w}^* = E\left[\underline{z}_j \underline{z}_j^T\right]^{-1} E\left[d_j \underline{z}_j\right] \tag{35}$$

Comparing equations (34) and (35), we see that n causes a bias in $\underline{w}^\circ$. From equation (34) it follows that $\underline{w}^\circ < \underline{w}^*$.

The effect of noise is also reflected in the weight update equation (eq. (31)), which can be expanded to

$$\Delta \underline{w}_j = 2\mu d_j (\underline{z}_j + \underline{n}_j) - 2\mu (\underline{z}_j + \underline{n}_j)(\underline{z}_j + \underline{n}_j)^T \underline{w}_j \tag{36}$$

in which the component due to the noise is

$$\Delta \underline{w}_{n_j} = 2\mu d_j \underline{n}_j - 2\mu (\underline{z}_j \underline{n}_j^T + \underline{n}_j \underline{z}_j^T + \underline{n}_j \underline{n}_j^T) \underline{w}_j \tag{37}$$

The noise also affects the filter output.

$$y_j = \underline{z}_{m_j}^T \underline{w}_j = (\underline{z}_j + \underline{n}_j)^T (\underline{w}^\circ + \Delta \underline{w}_{n_j}) \tag{38}$$

The component due to noise is

$$y_{n_j} = \underline{z}_j^T (\Delta \underline{w}_{n_j}) + \underline{n}_j^T (\underline{w}^\circ + \Delta \underline{w}_{n_j}) \tag{39}$$

If the misadjustment noise $\Delta\underline{w}_{m_j}$ due to M_w is included, the noise component of the filter output becomes

$$y_{n_j} = \underline{z}_j^T(\Delta\underline{w}_{m_j} + \Delta\underline{w}_{n_j}) + \underline{n}_j^T(\underline{w}^\circ + \Delta\underline{w}_{m_j} + \Delta\underline{w}_{n_j}) \tag{40}$$

Equation (40) shows that the effect of noise on y is very complex and is not simply additive.

Furthermore, equation (40) shows that the noise component y_{n_j} in y_j is a combination of additive and modulative terms. To reduce the intensity of noise in the system output z_{m_j} as well as to reduce its effect on biasing G, a scheme for noise suppression is investigated in the next section.

3 NOISE SUPPRESSION BY INVERSE MODELING

In section 2.5, the effect of system output noise n on the bias of the controller G was indicated. Such bias may affect the correct convergence $GP \rightarrow M$, and consequently distort the desired closed-loop response of T. For this reason, and because a fundamental objective is to suppress output noise, this issue is addressed in this section in conjunction with adaptive control.

3.1 Noise Characteristics in Linear Time Invariant Systems

Consider a stable, linear, time-invariant system described in SISO transfer function form $T_u(s)$ (fig. 5). The input is $u(t)$ and the corresponding response $z(t)$ is perturbed by output-referred additive noise $n(t)$. It is first assumed that $T_u(s)$ is completely known. It can represent a closed-loop system in which a time-invariant minimum phase plant $P(s)$ with relative degree $r(P) \geq 0$ is controlled by $G(s)$ (fig. 6). Measurement noise is represented by v and process noise by w.

$$T_u(s) = \frac{z_m(s)}{u(s)} = \frac{G(s)P(s)}{1 + G(s)P(s)} \tag{41}$$

Here $G(s)$ is chosen to fulfill two requirements :

$$1. \quad \lim_{s\to 0} T_u(s) = 1 \tag{42}$$

$$2. \quad r(T_u) \geq r(P) \tag{43}$$

where $r(T_u)$ is the relative degree of $T_u(s)$. Requirement 1 may imply integral control in $G(s)$. Requirement 2 implies physical realizability of $G(s)$, i.e.,

$$3. \quad r(G) \geq 0 \tag{44}$$

where $r(G)$ is the relative degree of $G(s)$.

The noise n due to v is given by :

$$n(s) = \frac{1}{1 + G(s)P(s)}\, v(s) = T_v(s)v(s) \tag{45}$$

and n due to w is

$$n(s) = \frac{P(s)}{1+G(s)P(s)}\, w(s) = T_w(s)w(s) \tag{46}$$

where $T_v(s)$ and $T_w(s)$ are the corresponding noise-transfer functions. We make the following assumptions :

1. The integral control implied by requirement 1 is of an order not greater than 1, i.e., not more than one open-loop pole at $s = 0$.
2. $r(G) = 0$. According to requirement 2, this implies $r(T_u) = r(P)$.
3. $r(P) > 0$.

The following observations can be made.

1. The design of $T(s)$ uniquely determines $T_v(s)$.
2. From equation (45), $r(T_v) = 0$ and from assumption 1, $T_v(s)$ has a zero at $s = 0$, implying $\lim_{s\to 0} T_v(s) = 0$, and with $r(T_v) = 0$, $\lim_{s\to\infty} T_v(s) = 1$. Thus, the low-frequency components due to $v(s)$ are attenuated in accordance with the slope of +20dB/decade. High-frequency components are not attenuated. Since the bandwidth of the control system is by far smaller than that of white measurement noise, $n(s)$ due to $v(s)$ is hardly affected by the control activity. On the other hand, $var(n)$, the variance of n, due to v is assumed to be negligibly small in its effect on biasing G.
3. From equation (46), $r(T_w) = r(P)$ and from assumption 1, $T_w(s)$ has a zero at $s = 0$ implying that $\lim_{s\to 0} T_w(s) = 0$ and that the low-frequency slope of $T_w(s)$ is +20dB/decade. It also implies that $\lim_{s\to\infty} T_w(s) = 0$ and the high-frequency slope is $-20r(P)$dB/decade.

In linear systems design, practical design considerations related to the constraints on control activity and to the lack of information on unmodeled modes impose limitations on the admissible loop-gain response GP and in view of equations (41), (45), and (46), on the noise suppression characteristics of the control system.

3.2 Principle of Noise Suppression by Error Feedback

In this section, the concept of noise suppression by error feedback in linear time-invariant systems is presented in two alternative forms. The analysis indicates the limitations of its practical implementation in linear time-invariant systems and shows the need for adaptive control.

Having assumed linear-time invariant systems, the Laplace operator s will be dropped for simplicity of notation. It is initially assumed that the closed-loop system T_u is completely known so that our exact model $T_m = T_u$ can be realized and its inverse T_m^{-1} can be formulated. However, since $r(T_u) > 1$, T_m^{-1} cannot be implemented as this would imply $r(T_m^{-1}) < 1$

which is not realizable. Instead, an approximate inverse $T_m^{-1}D$ having $r(T_m^{-1}D) = 0$ can be realized. The function D is a linear transfer function with $r(D) = r(T_u) > 1$ which satisfies

$$\lim_{s\to 0} D(s) = 1 \tag{47}$$

Consider now the system shown in figure 7. This feedback structure, also known as error feedback has been used in different applications whenever the problem is to suppress noise while avoiding any major effect on the principal input–output relationship.

Given that

$$\epsilon = z_m - x = T_u u_s + n - T_m u_s \tag{48}$$

$$u_s = u - T_m^{-1} D\epsilon \tag{49}$$

$$z_m = T_u u_s + n \tag{50}$$

and since $T_m^{-1}T_m = 1$ by definition, it is easily shown that :

$$z_m = \frac{T_u}{1 - D + T_m^{-1}T_u D}\, u + \frac{1 - D}{1 - D + T_m^{-1}T_u D}\, n \tag{51}$$

The scheme in figure 7 that yields equation (51) will be referred to as type I. Assuming that throughout the useful bandwidth of u and n, $D \cong 1$, and that $T_m^{-1}T_u = 1$, we have from equation (51)

$$z_m \cong T_m u \tag{52}$$

Thus, ideally the noise is cancelled and the response z_m is dictated by the model T_m, i.e., the noise cancellation does not interfere with the main transfer function T_u.

Equation (51) can be rewritten in a more familiar form by dividing numerators and denominators by $(1 - D)$. Thus

$$z_m = \frac{\frac{T_u}{1-D}}{1 + T_m^{-1}T_u \frac{D}{1-D}}\, u + \frac{1}{1 + T_m^{-1}T_u \frac{D}{1-D}}\, n \tag{53}$$

The equivalent scheme representing equation (53) is shown in figure 8. This formulation demonstrates that the attempt to implement $D \to 1$, is equivalent to requiring a large loop gain in figure 8. This may eventually cause instability. To illustrate this, consider the example:

$$D(s) = \frac{a_0}{s^2 + a_1 s + a_0} \tag{54}$$

Then,

$$\frac{D}{1 - D} = \frac{a_0}{s(s + a_1)} \tag{55}$$

which demonstrates that a_0, which determines the bandwidth of D, is also the feedback loop gain. In root locus representation, equation(55) indicates asymptotes at $\pm 90°$. Clearly, for a third-order $D(s)$, the asymptotes would be $\pm 60°$ and $180°$, indicating possible instability.

An alternative implementation (type II) of error feedback for noise suppression is shown in figure 9. With the relations,

$$\epsilon = z_m - x = T_u u_s + n - T_m u \tag{56}$$

$$u_s = u - T_m^{-1} D' \epsilon \tag{57}$$

$$z_m = T_u u_s + n \tag{58}$$

D' fulfills the same requirements as D except the requirement of equation (47). The solution of z_m from equations (56) to (58) is

$$z_m = \frac{T_u(1+D')}{1+T_m^{-1}T_u D'} u + \frac{1}{1+T_m^{-1}T_u D'} n \tag{59}$$

If $T_m^{-1}T_u = 1$ is fulfilled, the result is

$$z_m = T_u u + \frac{1}{1+D'} n \tag{60}$$

Thus, noise suppression is accomplished by a large gain of D' in the useful frequency range of n.

It is easily verified that in scheme type I, the noise suppression is accomplished by "pumping" n from z_m into x, whereas in type II the noise suppression is accomplished by the attenuation $(1+D')^{-1}$ as shown in equation (60). However, substituting

$$D' = \frac{D}{1-D} \tag{61}$$

equation (59) is changed to

$$z_m = T_u \frac{1+\frac{D}{1-D}}{1+T_m^{-1}T_u\frac{D}{1-D}} u + \frac{1}{1+T_m^{-1}T_u\frac{D}{1-D}} n = \frac{T_u}{1-D+T_m^{-1}T_u D} u + \frac{1-D}{1-D+T_m^{-1}T_u D} n \tag{62}$$

which is identical to equation (51). Thus, given the transformation (61), schemes type I and type II are identical with respect to T_u and to noise suppression.

Examination of either equations (51) or (59) discloses the following:

1. In order to assure the desired response $T_u(s) = z_m(s)/u(s)$, it is required that

$$T_m^{-1}T_u = 1 \tag{63}$$

2. If this requirement is fulfilled, it follows that

$$z_m = T_u u + (1-D)n \tag{64}$$

In general, when $T_u(s)$ is implemented by classical linear-feedback design as defined in equation (41), it cannot be made to provide the required robustness of T_u to fulfill condition (63) under large parameter variations in P. Thus, noise suppression, as derived by equation (51) or (59), is practically incompatible with conventional linear feedback design. However, in conjunction with the concept of MRAC, in which T_m is the reference model described in the Control System configuration section, condition (63) is assumed to be fulfilled throughout a wide range of parameter variations. Given this assumption, equation (64) can be assumed to be correct.

In section 3.1, it has been shown that $n(s)$, either due to process noise w or measurement noise v, has a high-pass slope of +20dB/decade at low frequencies. It is easily verified that with the assumptions placed on D, $(1 - D)$ has a +20dB/decade high pass slope. The consequence therefore is that with noise cancellation, the closed-loop system, in accordance with figure 7 or figure 9, now has a +40dB per decade slope with respect to noise. Furthermore, the frequency breakpoint of D can be made considerably higher than that of T_u. Since, as is evident from equation (46), n due to w is mostly a filtered low-frequency process, the high pass filtering by $(1 - D)n$ in equation (64) can contribute to substantial suppression of process noise.

3.3 Example of Noise Suppression

In this section, the effect of noise suppression is demonstrated by a numerical example. Assume a plant P with $r(P) = 2$, given by

$$P(s) = \frac{a_{p_0}}{s^2 + a_{p_1}s + a_{p_0}} \tag{65}$$

Let $r(T_m) = r(P) = 2$, and let T_m be

$$T_m(s) = \frac{s + a_{m_0}}{s^3 + a_{m_2}s^2 + a_{m_1}s + a_{m_0}} \tag{66}$$

Then, with $r(D) = r(T_m) = 2$, and let $D(s)$ be

$$D(s) = \frac{d_0}{s^2 + d_1 s + d_0} \tag{67}$$

The open-loop transfer function according to equation (8) is:

$$G_i(s)M(s) = \frac{T_m(s)}{1 - T_m(s)} = \frac{s + a_{m_0}}{s} \frac{1}{s^2 + a_{m_2}s + a_{m_1} - 1} \tag{68}$$

with

$$G_i(s) = \frac{s + a_{m_0}}{s} \tag{69}$$

$$M(s) = \frac{1}{s^2 + a_{m_2}s + a_{m_1} - 1} \tag{70}$$

The function $G_i(s)$ is not incorporated in the open-loop reference model $M(s)$ because the integrator would have required an infinitely long FIR. Instead G_i is incorporated into the closed-loop system as a series compensator in accordance with figure 4 (see Section 2.2). Since in the adapted system $GP \rightarrow M$, we have, in accordance with equation (46),

$$n(s) = \frac{P(s)}{1 + G_i(s)M(s)} w(s) = \frac{a_{p_0}(s^2 + a_{m_2}s + a_{m_1} - 1)}{(s^2 + a_{p_1}s + a_{p_0})(s^3 + a_{m_2}s^2 + a_{m_1}s + a_{m_0})} w(s) \tag{71}$$

The following values are chosen:

P : $a_{p_0} = 25$; $a_{p_1} = 1$

T_m : $a_{m_0} = 10$; $a_{m_1} = 10$; $a_{m_2} = 6.5$

D : $d_0 = 150$; $d_1 = 20$

The plant P with the above values will be referred to as the FAST plant. The process noise $w(s)$ is chosen as zero-mean white noise with unity Power Spectral Density (PSD). The variance of $n(s)$, with the above numerical values for P, T_m, and D is

$$var(n) = 14.722 \tag{72}$$

In accordance with equation (64), the suppressed noise is

$$n_s = (1 - D)n \tag{73}$$

and explicitly

$$n_s = \frac{a_{p_0} s^2 (s^2 + a_{m_2} s + a_{m_1} - 1)(s + d_1)}{(s^2 + a_{p_1} s + a_{p_0})(s^3 + a_{m_2} s^2 + a_{m_1} s + a_{m_0})(s^2 + d_1 s + d_0)} w(s) \tag{74}$$

With the above numerical values

$$var(n_s) = 5.8359 \tag{75}$$

The ratio α of the rms values of n and n_s is

$$\alpha = \left(\frac{var(n_s)}{var(n)}\right)^{1/2} = 0.62 \tag{76}$$

This result implies that because of the relatively high frequency of the resonant peak of n_s, $w \cong \sqrt{a_{p_0}} = 5\, rad$, n is not substantially suppressed by the noise cancellation scheme. However, if $a_{p_0} = 4$, referred to as the SLOW plant, and all the other numerical values are unchanged, the result is

$$var(n) = 3.104 \tag{77}$$

$$var(n_s) = 0.219 \tag{78}$$

and α is,

$$\alpha = 0.265 \tag{79}$$

which is a substantial-noise suppression. The low-frequency approximate transfer functions without and with noise suppression as derived from equations (71) and (74) are correspondingly:

$$\frac{n(s)}{w(s)} \cong \frac{s(a_{m_1} - 1)}{a_{m_0}} \tag{80}$$

$$\frac{n_s(s)}{w(s)} \cong \frac{s^2(a_{m_1} - 1)}{a_{m_0}} \frac{d_1}{d_0} \tag{81}$$

Equations (80) and (81) emphasize the trend indicated by the results given in equations (72), (75), (77), and (78) accordingly. Figures 10 and 11 show the frequency-response plots of equations (71) and (74) for the corresponding plant parameters $a_{p_0} = 25$ and $a_{p_0} = 4$ and also show the levels of noise suppression that are achieved in the two cases.

4 REALIZATION OF NOISE SUPPRESSION

In section 3, suppression of additive noise by error feedback (shown in fig. 7) is presented for a linear system. For the fulfillment of condition (63), it is required that T_u adapt so that $T_u \rightarrow T_m$. However, in view of equation (30) of ([10]), the additive-output noise n excites weight noise in addition to the intrinsic misadjustment noise in $\underline{w}_j$. This noise is modulative and it combines with n in a highly complex nonlinear manner. Consequently, noise suppression by linear error feedback as presented in section 3 cannot be as effective as that predicted by linear analysis, unless the adaptation gain, $\mu = (ftr(R))^{-1} \ll 1$, which implies a very slow rate of adaptation. This conflict between the rate of adaptation and weight noise is a problem which cannot be resolved in basic estimators such as LMS or RLS. However, by introducing a modified LMS algorithm in which the adaptation gain μ is monotonically related to a suitable measure of the adaptation error e, this conflict can be resolved to a substantial degree.

4.1 Variable-Gain LMS Filter

The parameters of the controlled plant $P(s)$ are regarded as piecewise-constant time processes, i.e., at random times, any plant parameter may undergo an abrupt step-change to a new unknown value. It is required that the adaptive algorithm adjusts the controller G to the new value of P so as to enforce $GP \rightarrow M$ as rapidly as possible. This implies that μ should be assigned the largest permitted value $\mu_0 = (tr(R))^{-1}$. On the other hand, during the quiescent time intervals, μ should be vanishingly small so as to reduce weight noise due to n or to misadjustment. In equation (3), e_j represents the adaptation error. Its squared averaged value is used to determine μ as follows: Let

$$\mu_0 = (ftr(R_j))^{-1} \tag{82}$$

where $f \geq 1$ so as to fulfill the stability condition $0 < \mu_0 < (tr(R_j))^{-1}$ and let

$$\overline{e_j^2} = \sum_{j=1}^{N'} e_j^2 \tag{83}$$

where $N' \leq N$, and N is the number of lags in the LMS delay line. Define

$$\varepsilon_j \triangleq \left(\frac{\overline{e_j^2}}{tr(R_j)} \right)^{1/2} \tag{84}$$

We now choose a monotonic function $\mu = \mu(\varepsilon)$ as follows. Let ε_t and ε_s be the threshold and saturation points respectively, of ε. Then, the actual μ in the LMS is given by:

$$\mu_j = \begin{cases} 0 & ; 0 \leq \varepsilon_j < \varepsilon_t \\ \dfrac{\varepsilon_j - \varepsilon_t}{\varepsilon_s - \varepsilon_t} \mu_0 & ; \varepsilon_t \leq \varepsilon_j < \varepsilon_s \\ \mu_0 & ; \varepsilon_j \geq \varepsilon_s \end{cases} \tag{85}$$

Equation (85) is illustrated in figure 12. Thus, the initial convergence after a step change in plant parameters is determined by μ_0. For example, for $f = 2$, in accordance with

equation (24), the initial time constant of convergence in terms of the number of iterations is

$$\tau = \frac{fN}{4} = \frac{N}{2} \tag{86}$$

as long as $\varepsilon \geq \varepsilon_s$. The convergence rate then slows down with the decreasing value of μ. Eventually when $\varepsilon < \varepsilon_t$, the weight noise vanishes and the algorithm effectively discontinues the weight updating in accordance with equation (85). Furthermore, ε_t can be set so that during the quiescent periods, $\varepsilon < \varepsilon_t$ is maintained even in the presence of noise n. The consequence is that the introduction of the threshold ε_t inhibits the excitation of parameter noise. Accordingly, with the variable-gain LMS, the system output noise essentially retains its additive nature. Therefore noise suppression by linear error feedback can retain its effectiveness as presented in section 3. However, if plant parameters vary continuously and at relatively high rates, $\overline{e^2}$, and therefore ε, cannot become small, so substantial parameter noise, and consequently system noise, will be present.

4.2 System Description

The complete adaptive-control system, incorporating noise suppression by error feedback in accordance with section 3, and variable adaptation gain $\mu = \mu(\varepsilon)$ (not explicitly shown), is described in figure 13. The two versions of error feedback, described in section 3.2, namely Type I and Type II are indicated by the solid and dashed lines, respectively. The reference model T_r is the same as T_m, and its response to u, z_r, is used for comparison with the actual system output z. The variable e is the adaptation error driving the gradient algorithm in accordance with equation (7); ϵ is the system error in accordance with equation (48) used for noise suppression, and n_c is the output of the noise suppression loop.

5 COMPUTER SIMULATIONS

The results of the simulation tests presented in this section illustrate the concepts discussed in the previous sections. In particular, the examples demonstrate 1) the performance of the system without the improvements presented in this paper, 2) the effects of using the variable gain algorithm, and 3) the noise suppression scheme.

5.1 Implementation

The following parameters were used in the simulation tests.

1. For the majority of the examples, the "unknown" plant was

$$P(s) = \frac{25}{s^2 + s + 25}$$

which has a natural frequency $\omega \cong 5$ and a damping factor $\varsigma = 0.1$. This plant is occasionally referred to as the FAST plant. In some examples, a step change in gain

occurs. The plant after the step change is

$$P(s) = \frac{50}{s^2 + s + 25}$$

There are also a couple of examples which use a SLOW plant. These use

$$P(s) = \frac{4}{s^2 + s + 4}$$

which has a natural frequency $\omega \cong 2$ and a damping factor $\zeta = 0.25$

2. The closed-loop reference model was

$$T(s) = \frac{s + 10}{s^3 + 6.5s^2 + 10s + 10}$$

and the open-loop reference model was

$$M(s) = \frac{10}{s^2 + 6.5s + 9}$$

3. The input control signal u was a square wave with an amplitude of 1 and a period of 10 sec.

4. The integral controller $G_i(s)$ was

$$G_i(s) = \frac{0.1(s + 10)}{s}$$

5. For the runs which included the noise suppression scheme, the filter $D(s)$ was

$$D(s) = \frac{150}{s^2 + 20s + 150}$$

6. All initial conditions of the various systems were set to zero. The initial weights of the controllers G and G_c were

$$w_i = \begin{cases} 1 & i = 0 \\ 0 & i = 1, \ldots, N \end{cases}$$

Note that if all the weights of the controllers are zero, the system cannot start because no signal gets past the G_c. The above choice of weights is arbitrary.

7. The parameters for the variable gain scheme were

$$\begin{aligned} \varepsilon_t &= 0.05 \\ \varepsilon_s &= 1.00 \\ f &= 2 \end{aligned}$$

8. The filter parameters were 21 weights ($N = 21$) and the tap spacing was 0.1 sec ($\Delta T = 0.1$), resulting in a filter with $T_f = 2.0$ sec. These parameters were calculated using equations (16)–(19) and $M(s)$ of item 2.

9. The weights of the controllers G and G_c were updated every ΔT sec.

10. In all cases, all of the blocks (see block diagram, fig. 13) except for the controllers G and G_c, were modelled in continuous time. A sixth-order Runge-Kutta integration scheme was used with an integration step size of $dt = 0.002$ sec. The outputs of G and G_c were also calculated every dt sec.

11. When included, the process noise w was zero-mean white noise, with a standard deviation σ_w of 0.2, and was sampled every dt sec.

12. The simulations were run for 50 sec (25,000 iterations).

5.2 Results

Table 1 summarizes the various configurations used in the eight simulation runs; the results are presented in figures 14-21.

Run 1 has the traditional LMS filter, with a constant μ and $f = 2$; its results are shown in figure 14. Figure 14a, which compares the actual and reference responses, demonstrates poor performance. It also shows the nonlinearity of the system with the response to positive steps in the input being very different than the response to negative steps. Figure 14b shows the time history of some of the filter weights. As expected with the high gain ($f = 2$), the weights are very noisy.

A smaller gain ($f = 10$) is used with a constant μ in run 2, figure 15. Comparing figure 15a with figure 14a, we note a considerable reduction in the weight noise. A step change in the plant gain, doubled from 1 to 2, occurs at 27.5 sec. The system adapts to this plant change, although the adaptation rate is relatively slow. Figure 15b shows the time history of some of the filter weights. It shows that the weights responded to the plant change. The weights are much less noisy than in figure 14b.

The variable μ scheme is introduced in run 3. Figure 16a shows that the system performance is quite similar to that of run 2, of figure 15a. However, the plot of the weights, figure 16b, shows that the weights, once settled, are almost noise-free. Comparing this with figure 15b, the advantage of the variable-gain LMS is clear. However, the penalty one pays for shutting off the adaptation (i.e., when $\varepsilon < \varepsilon_t$) can be seen in the final section of Figure 16(a). The adaptation has stopped after 33 sec because the filter error is small, but the error in the system response is still noticeable. This can be improved by reducing the threshold ε_t in the variable μ scheme.

In run 4 the noise suppression scheme is included. However, no process or measurement noise is introduced, and therefore the noise suppression loop can be regarded as simply providing additional feedback. The system performance as shown in figure 17a has improved considerably compared with figure 16a. Furthermore, the transient caused by the plant change at 27.5 sec is much better than in run 3. Figure 17b, the time history of the filter weights, shows that the weights initially responded slightly more slowly than the corresponding change in figure 16b. This is caused by the noise suppression loop, which modifies u to u_s. The signal u_s excites the adaptive scheme to a lesser extent than u. Figure 17(c) shows the output of the noise suppression loop (n_c in fig. 13). The significance of figure 17c will be discussed in section 5.3. Finally, figure 17d shows e_z, the error in the

system output ($e_z = z_r - z$), for runs 3 and 4. The dotted line is for run 3, without the noise suppression loop, and the solid line is for run 4, with noise suppression.

In run 5, process noise is added. The noise w is zero-mean white noise with standard deviation $\sigma_w = 0.2$ and is sampled every dt sec ($dt = 0.002$). The noise suppression loop is not used in run 5. Figure 18a shows the actual and reference system output and figure 18b shows the time history of some of the filter weights. In spite of the presence of process noise, the weight noise is negligible. However, the process noise clearly corrupts the system output. In run 6, the same process noise was added, but the noise suppression loop was used. These results are shown in figures 19a and 19b. As expected, the effect of the process noise on the system output is much smaller in run 6. Figure 19c compares e_z for runs 5 and 6.

In runs 7 and 8, the SLOW plant is used, without and with noise suppression, respectively, with the same process noise ($\sigma_w = 0.2$) as in runs 5 and 6. Figures 20 and 21a show the system responses in the two cases. Figure 21b shows the error e_z for the two cases.

5.3 Discussion

In the configuration of runs 4, 6, and 8 there are in essence two feedback loops, the adaptive controller G and the noise suppression loop. It is important to note the differences in their roles. The adaptive controller has to adjust itself (its weights) such that $PG \rightarrow M$. The noise suppression loop has to minimize the undesired perturbations in system response caused by noise and other disturbances. For run 4, figure 17c shows the output of the noise suppression loop (n_c in fig. 13). Clearly, the large peak caused by the plant change occurs before G has had time to adjust. As G adjusts, the noise suppression loop returns to its normal level of performance. This demonstrates that the two feedback loops are fulfilling their distinct roles and not interfering with each other.

To compare the simulation results with the analysis of section 3, the root mean square (rms) values of e_z were calculated. These are presented in table 2. For runs 3 and 4, $rms(e_z)$ was calculated over the range 5 to 25 sec — after the initial transient had vanished and before the jump in plant gain had occurred. For runs 5 and 6, the range 5 to 50 sec was used. For runs 7 and 8, the range 10 to 50 sec was used. Comparing run 3 with 4, run 5 with 6, and run 7 with 8 shows that in each case the addition of the noise suppression decreased the error e_z by more than a factor of 3.

We note that there is an increase in the system error e_z from runs 3 and 4 to runs 5 and 6. This increase is caused by the addition of process noise w. The error due to w is statistically independent of the the error from other causes (primarily the mismatch between PG and M). We can now calculate the noise at the output due to process noise. By adding subscripts to e_z to refer to run numbers, and given that n and n_s represent output-referred noise without and with noise suppression, respectively (from section 3.3)

$$\sigma_n = \sqrt{\sigma^2_{e_{z_5}} - \sigma^2_{e_{z_3}}} = 0.042 \tag{87}$$

$$\sigma_{n_s} = \sqrt{\sigma^2_{e_{z_6}} - \sigma^2_{e_{z_4}}} = 0.015 \tag{88}$$

The analysis of section 3.3, which assumed that the noise w had a unity PSD, resulted in (from equations (72) and (75))

$$\begin{aligned} var(n) &= 14.722 \\ var(n_s) &= 5.8359 \end{aligned} \tag{89}$$

The PSD of w used in the simulation is approximately given by

$$\text{PSD}(w) \simeq \sigma_w^2 * dt = (0.2)^2 * (0.002) = 0.00008 \tag{90}$$

The predicted values of σ_n and σ_{n_s} are therefore given by

$$\sigma_n = \sqrt{\text{PSD}(w) * var(n)} = 0.0343 \tag{91}$$

$$\sigma_{n_s} = \sqrt{\text{PSD}(w) * var(n_s)} = 0.0216 \tag{92}$$

These values are close to the simulation results of equations (87) and (88). For the results to match the analysis exactly, $\sigma_{e_{z_5}}$ should be smaller by 5% and $\sigma_{e_{z_6}}$ should be 12% larger. These small errors can be attributed to two main causes. The first is that equation (90) is an approximation. Secondly, the sample size is small. The number of statistically independent samples in e_z which have a dominant frequency of 5 rad/sec (the lightly damped mode of the plant) in a run of 50 sec is about 50. Therefore in runs 3 and 4 there are only about 20 independent samples. In view of these two points, the match between the analysis and simulation can be considered to be very good.

Runs 7 and 8 with the SLOW plant are equivalent to runs 5 and 6 with the FAST plant. Two more runs with the SLOW plant, equivalent to runs 3 and 4, were conducted (but not presented here) to calculate the effect of the noise. The results were

$$\sigma_n = 0.011 \tag{93}$$

$$\sigma_{n_s} = 0.003 \tag{94}$$

The predicted values are

$$\sigma_n = 0.0158 \tag{95}$$

$$\sigma_{n_s} = 0.0013 \tag{96}$$

These are very close to the simulation results. A change of only 2% in $\sigma_{e_{z_7}}$ and $\sigma_{e_{z_8}}$ would make the results match exactly.

The measure of the effectiveness of noise suppression developed in section 3.3 is

$$\alpha = \left(\frac{\sigma_{n_s}}{\sigma_n}\right) \tag{97}$$

For the FAST plant, use of equations (87) and (88) gives the result $\alpha = 0.36$, meaning that the noise suppression scheme reduced the effect of process noise w by about 64%. This is much better than the predicted value of $\alpha = 0.62$ from equation (76). The reason for the better-than-predicted performance is that the noise suppression scheme and the adaptive controller reinforce each other. The reduced level of noise leads to a more accurate G, which in turn leads to better noise suppression. This constructive interaction between the two feedback loops is one of the major advantages of the the total system.

To demonstrate, let α_p be the predicted value of α which is based on an assumption of a perfect $G = G_p$:

$$\alpha_p = \left(\frac{\sigma_{n_s}(G_p)}{\sigma_n(G_p)} \right) \tag{98}$$

By contrast, α_s, the simulation result, is formed from one run with noise suppression producing a "good" G, G_g, and one run without noise suppression producing a "fair" G, G_f:

$$\alpha_s = \left(\frac{\sigma_{n_s}(G_g)}{\sigma_n(G_f)} \right) \tag{99}$$

Note that α_p uses the same G for both its numerator and denominator. Assume that α_p is a good prediction if the G is consistent. Then, using G_f

$$\alpha_p = \left(\frac{\sigma_{n_s}(G_f)}{\sigma_n(G_f)} \right) \tag{100}$$

Since G_g is better than G_f

$$\frac{\sigma_{n_s}(G_g)}{\sigma_n(G_f)} < \frac{\sigma_{n_s}(G_f)}{\sigma_n(G_f)} \tag{101}$$

or

$$\alpha_s < \alpha_p \tag{102}$$

This qualitative analysis leads to the conclusion that α_s will be lower than α_p; the noise suppression will be more effective than predicted because of the improvement in G.

For the SLOW plant, the simulation result was $\alpha = 0.24$. The noise suppression was able to reduce the effect of the process noise by about 76%. This is very close to the predicted value of $\alpha = 0.265$ from equation (79). Again, the simulation results are better than predicted. In this case the difference is small because the system was able to converge to the correct value of G even without the noise suppression loop.

6 CONCLUSIONS

It has been shown that an adaptive filter can perform as a nonparametric controller in a closed-loop system. Although the error equation in the closed-loop system is not strictly linear, the system converges so as to establish a linear error equation in the adapted system. In the system discussed in this paper, the adaptive element is essentially an LMS filter. A variable gain scheme was introduced in which the gradient gain is a monotonic function of the adaptation error of the controller. This made it possible to have fast adaptation without large misadjustment noise. A model-inverse noise suppression scheme was also introduced. The noise-suppression and variable-gain schemes worked together in a mutually beneficial way to provide excellent noise suppression, system tracking, and response to plant changes.

In the present system, the elements of the input vector to the adaptive filter are not orthogonal. It is anticipated that a substantial reduction in the adaptation time can be achieved by an adaptive filter based on an orthogonalized input vector, such as recursive least squares or lattice filters, with successful implementation of an adaptive forgetting factor.

References

[1] Friedland, B.: Control System Design, an Introduction to State Space Methods. McGraw-Hill, 1986.

[2] Astrom, K. J.: Theory and Applications of Adaptive Control — A Survey. Automatica, vol. 19, no. 5, 1983, pp. 471–486.

[3] Goodwin, Graham C.; and Sin, Kwai Sang: Adaptive Filtering Prediction and Control. Prentice-Hall, Inc., Englewood Cliffs, NJ, 1984.

[4] Morse, A. S.: Global Stability of Parameter Adaptive Control Systems. IEEE Trans. on Automatic Control, vol. A-C 25, no. 3, June 1980, pp. 433–470.

[5] Widrow, B.; McCool, J. M.; Larimore, M. G.; and Johnson, C. R.: Stationary and Nonstationary Learning Characteristics of the LMS Adaptive Filter. Proceedings of the IEEE, vol. 64, no. 8, Aug. 1976, pp. 1151–1162.

[6] Cowan, C. F. N.; and Grant, P. M.: Adaptive Filters. Prentice-Hall, 1985.

[7] Widrow, B.; Glover, J. R.; McCool, J. M.; Kaunitz, J.; Williams, L. S.; Hearn, R. H.; Zeidler, J. R.; Dong, E.; and Goodlin, R. C.: Adaptive Noise Cancelling: Principles and Applications. Proc. IEEE, vol. 63, no. 12, Dec. 1975, pp. 1692–1716.

[8] Velger, M.; Grunwald, A.; and Merhav, S.: Suppression of Biodynamic Disturbances and Pilot Induced Oscillations by Adaptive Filtering. AIAA J. of Guidance, Control and Dynamics, vol. 7, no. 4, Aug. 1984, pp. 223–230.

[9] Velger, M.; Merhav, S. J.; and Grunwald, A.: Adaptive Filtering of Biodynamic Stick Feedthrough in Manipulation Tasks On Board Moving Platforms. AIAA Paper 86-2248CP, Williamsburg, VA, 1986.

[10] Merhav, S. J.: Design of Adaptive Control Systems by Means of Self-Adjusting Transversal Filters. NASA TM-86843, Feb. 1986.

[11] Mehta, R. S.; and Merhav, S. J.: Performance Characteristics of an Adaptive Controller Based on Least-Mean-Square Filters. AIAA Paper 86-2160CP, Williamsburg, VA, 1986.

[12] Widrow, B.; and Walach, E.: Adaptive Signal Processing For Adaptive Control. IFAC Workshop on Adaptive Systems in Control and Signal Processing, San Francisco, June 1983.

[13] Eleftheriou, E.; and Falconer, D. D.: Tracking Properties and Steady-State Performance of RLS Adaptive Filter Algorithms. IEEE Trans. on Acoustics, Speech, and Signal Processing, vol. ASSP-34, no. 5, Oct. 1986.

[14] Cioffi, J. M.; and Kailath, T.: Fast Recursive-Least-Squares Transversal Filters for Adaptive Filtering. IEEE Trans. on Acoustics, Speech and Signal Processing, vol. ASSP-32, April 1984, pp.304–337.

TABLE 1.– SIMULATION RUNS

Run No.	Constant or variable μ	f	σ_w	Noise suppression	Step change	Plant	Figures
1	C	2	0	No	No	FAST	14a,b
2	C	10	0	No	Yes	FAST	15a,b
3	V	2	0	No	Yes	FAST	16a,b; 17d
4	V	2	0	Yes	Yes	FAST	17a,b,c,d
5	V	2	0.2	No	No	FAST	18a,b; 19c
6	V	2	0.2	Yes	No	FAST	19a,b,c
7	V	2	0.2	No	No	SLOW	20; 21b
8	V	2	0.2	Yes	No	SLOW	21a,b

TABLE 2.– ERROR IN SYSTEM OUTPUT FOR RUNS 3 TO 8

Run No.	$rms(e_z)$
3	0.104
4	0.026
5	0.112
6	0.030
7	0.052
8	0.013

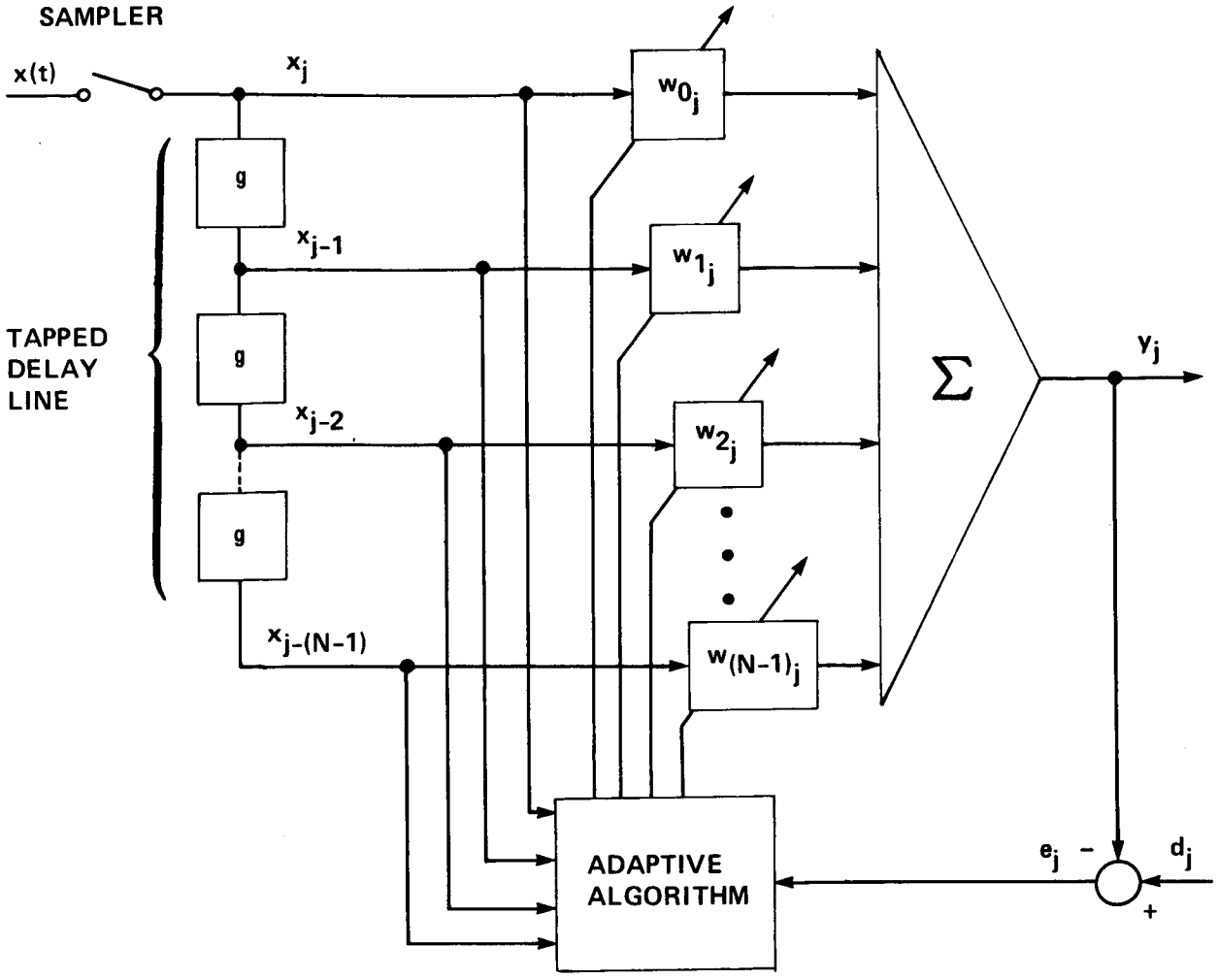

Figure 1.– Adaptive finite-impulse-response model.

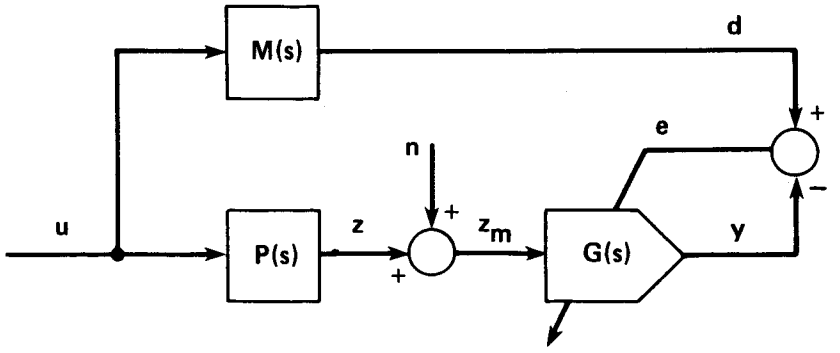

Figure 2.– MRAC adaptive element.

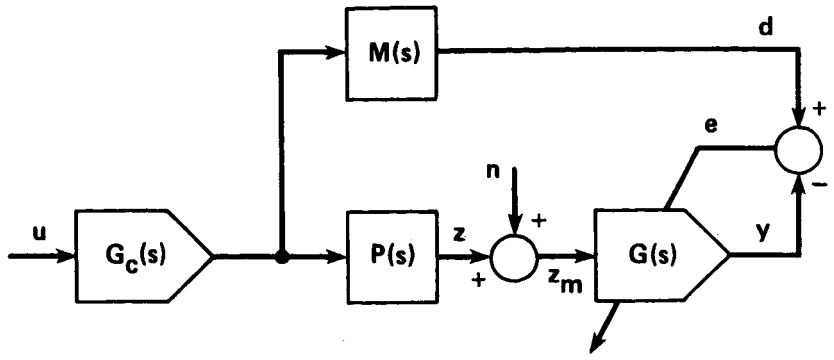

Figure 3.– Open-loop control system.

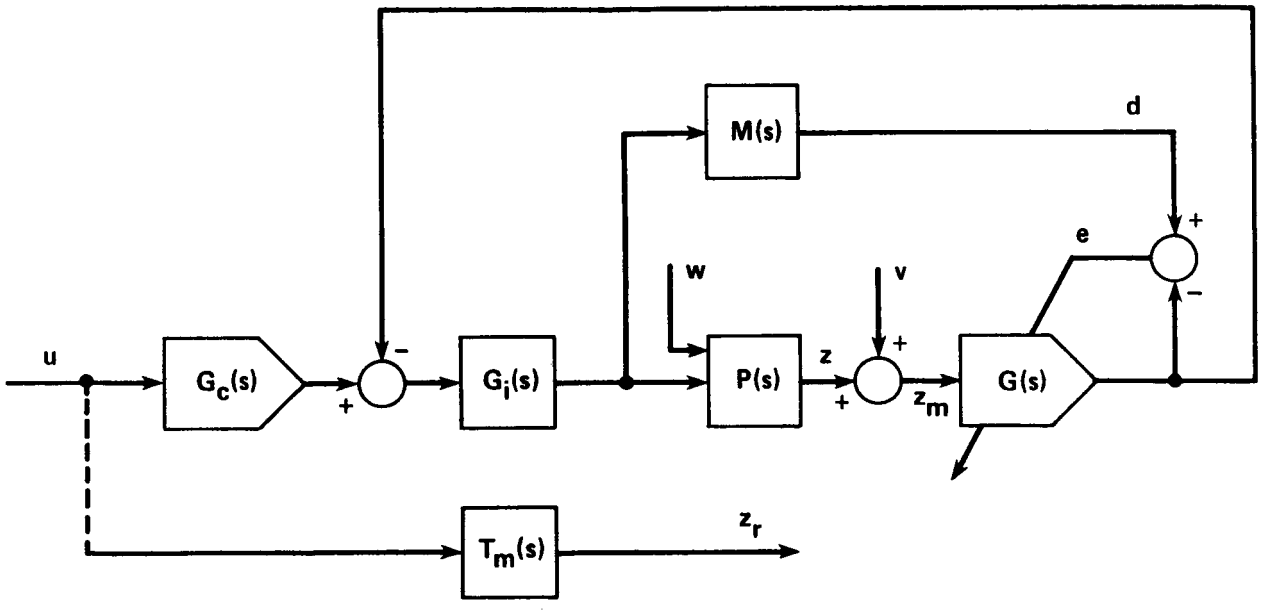

Figure 4.– Closed-loop control system.

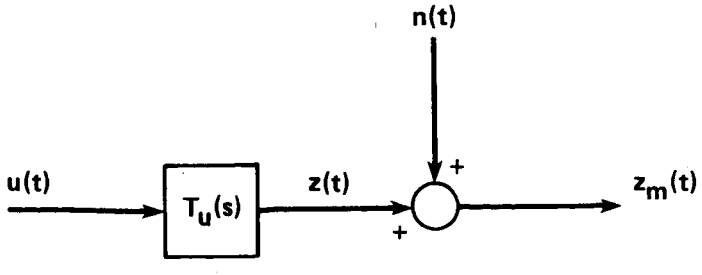

Figure 5.– SISO system.

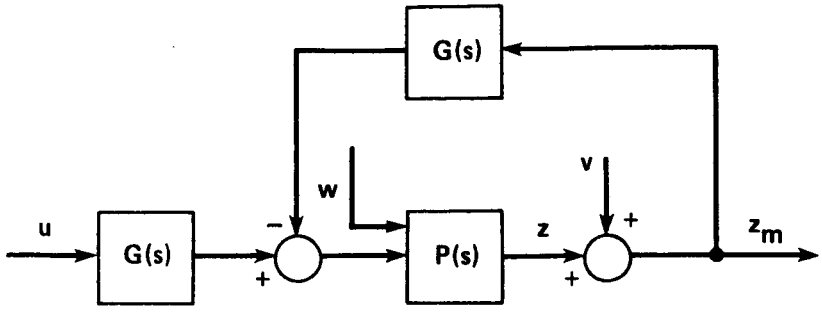

Figure 6.– Closed-loop system.

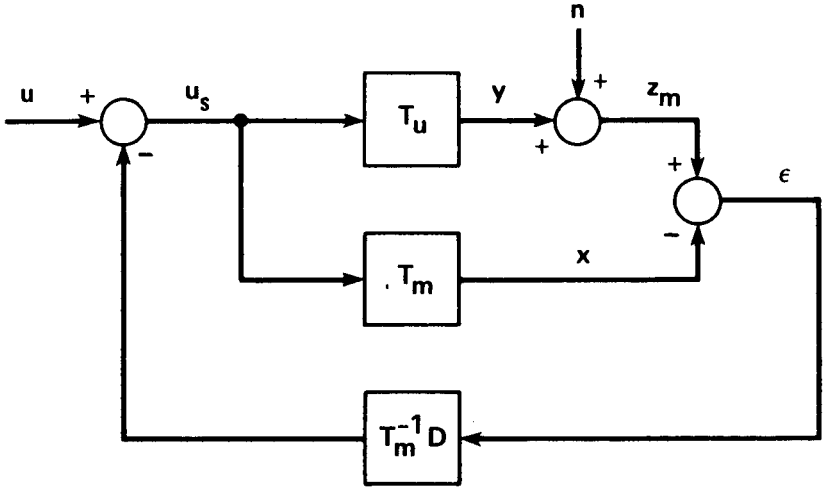

Figure 7.– Scheme for noise suppression by error feedback, type I.

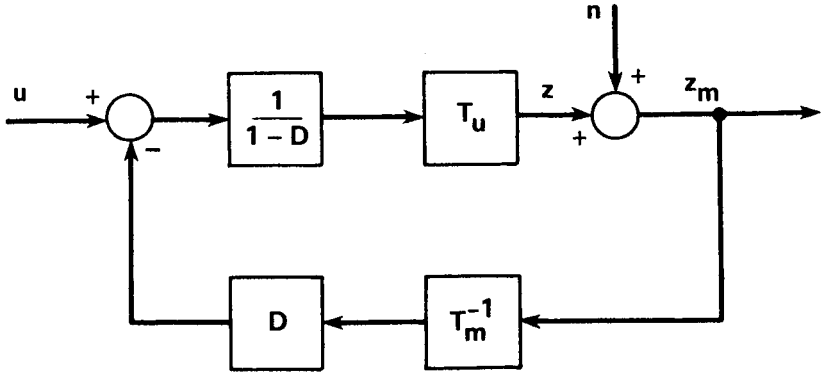

Figure 8.– Equivalent scheme for noise suppression, type I.

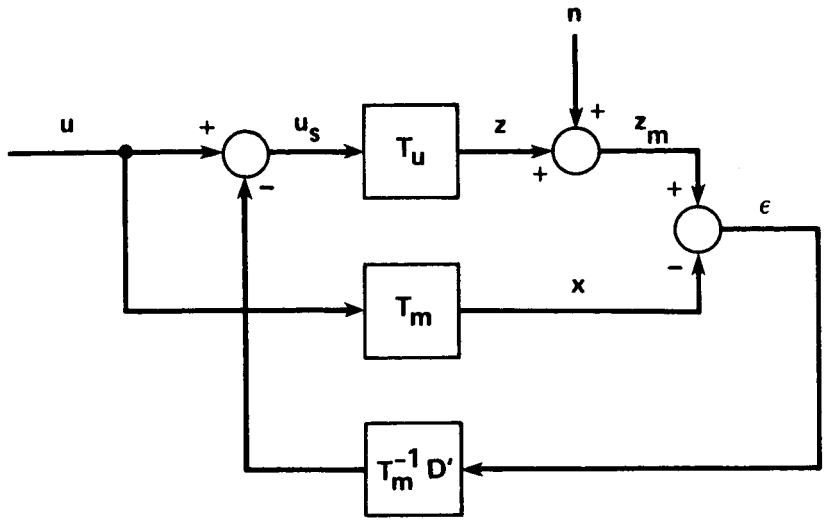

Figure 9.– Scheme for noise suppression by error feedback, type II.

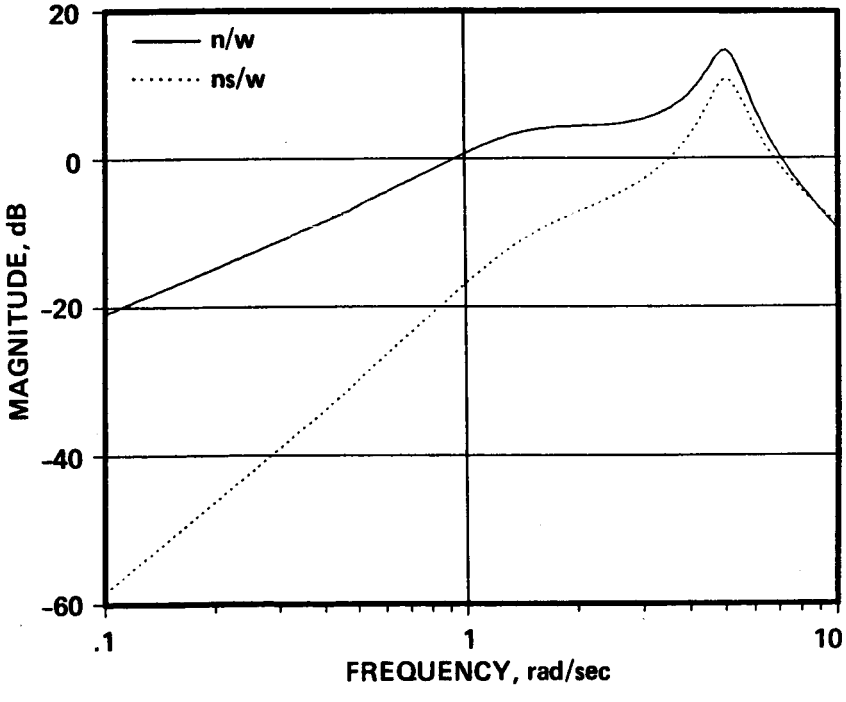

Figure 10.– Bode magnitude plot for output noise to input noise transfer function, FAST plant.

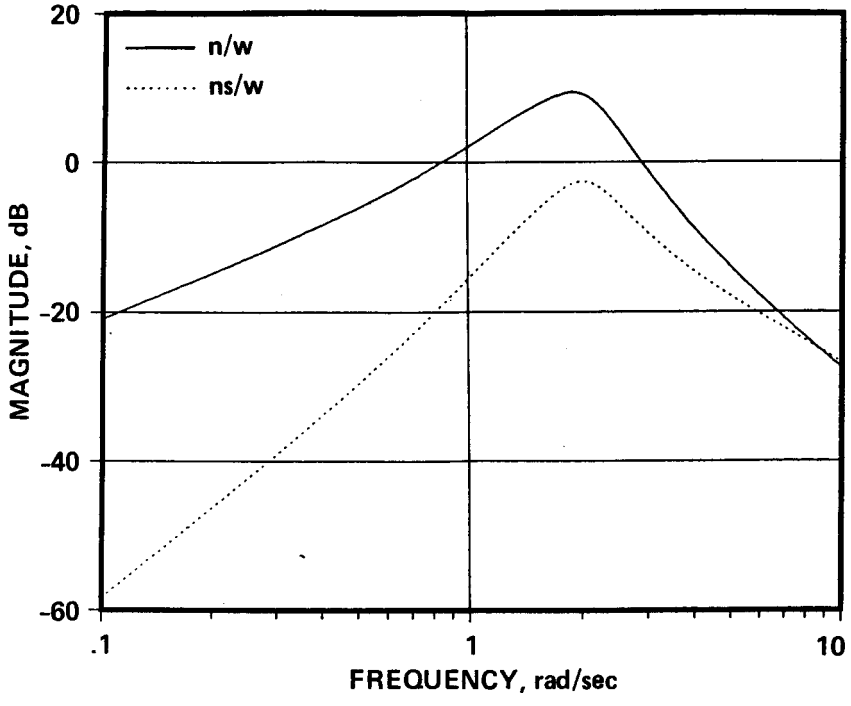

Figure 11.– Bode magnitude plot for output noise to input noise transfer function, SLOW plant.

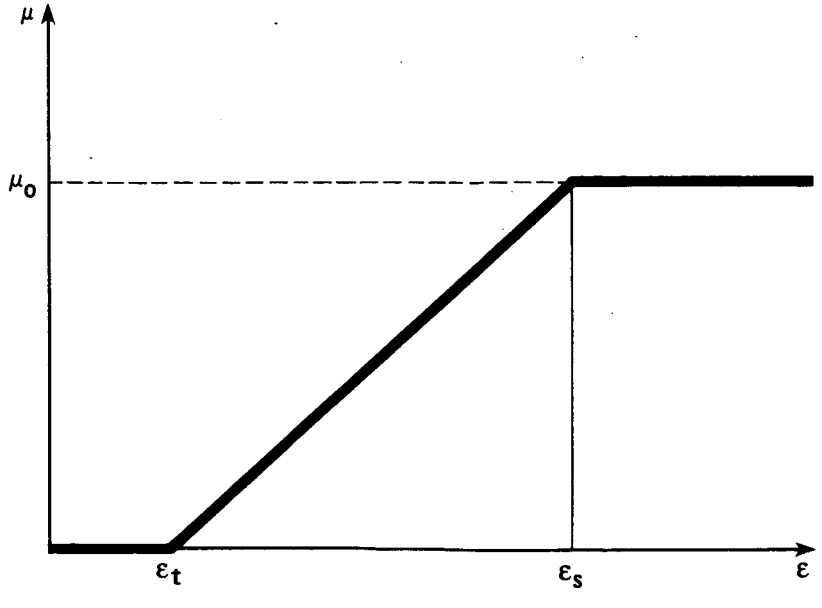

Figure 12.– Adaptation gain as a function of a measure of filter error.

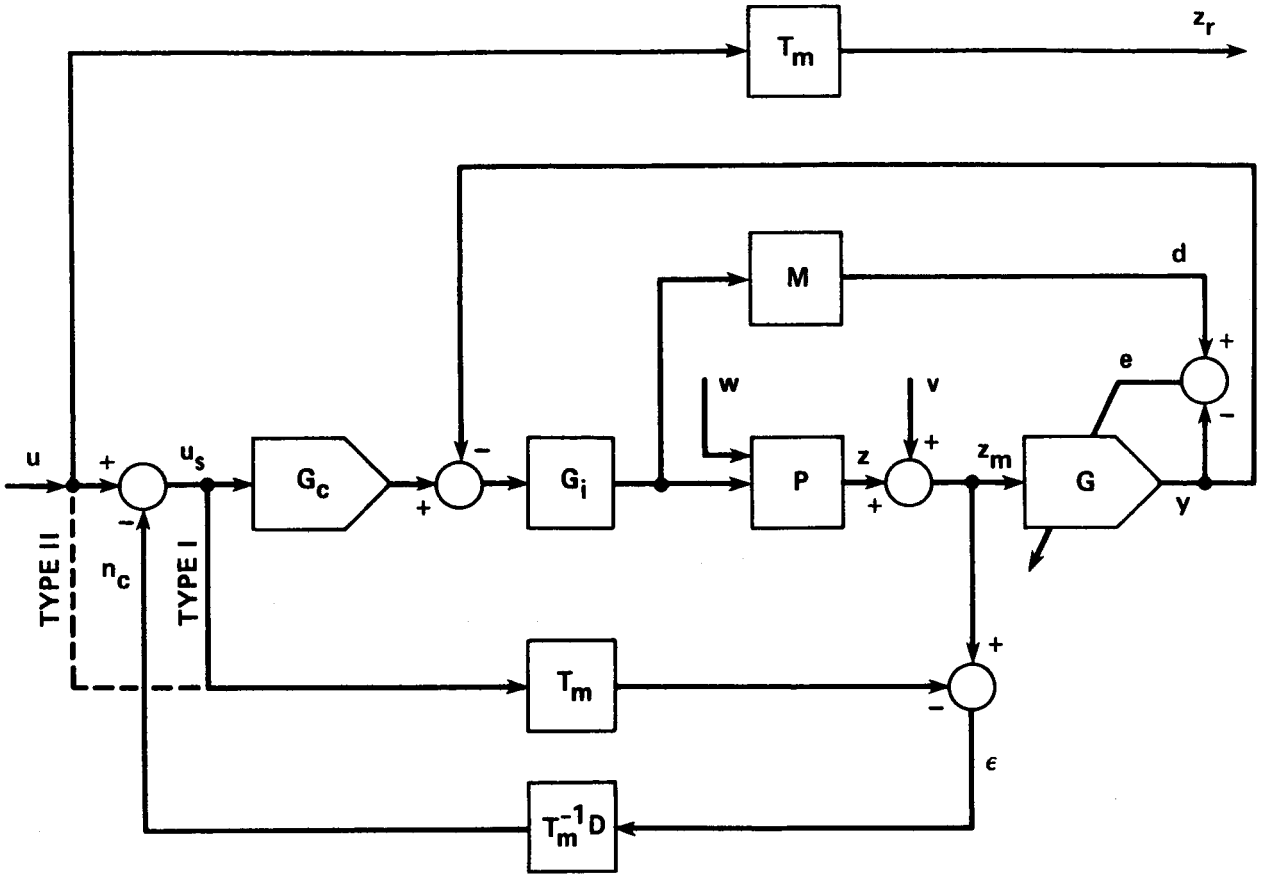

Figure 13.– Closed-loop control system with noise suppression.

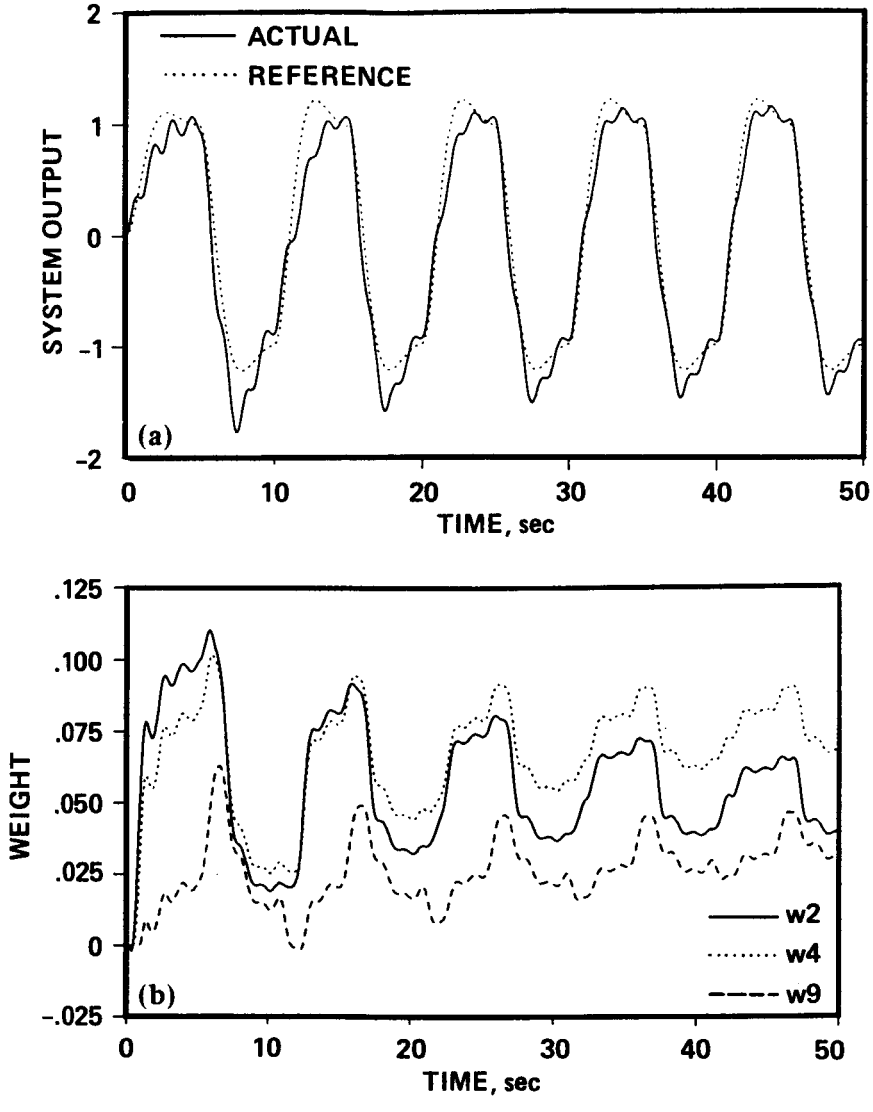

Figure 14.– Results of Run 1. (a) Actual and reference system output. (b) Time history of some filter weights.

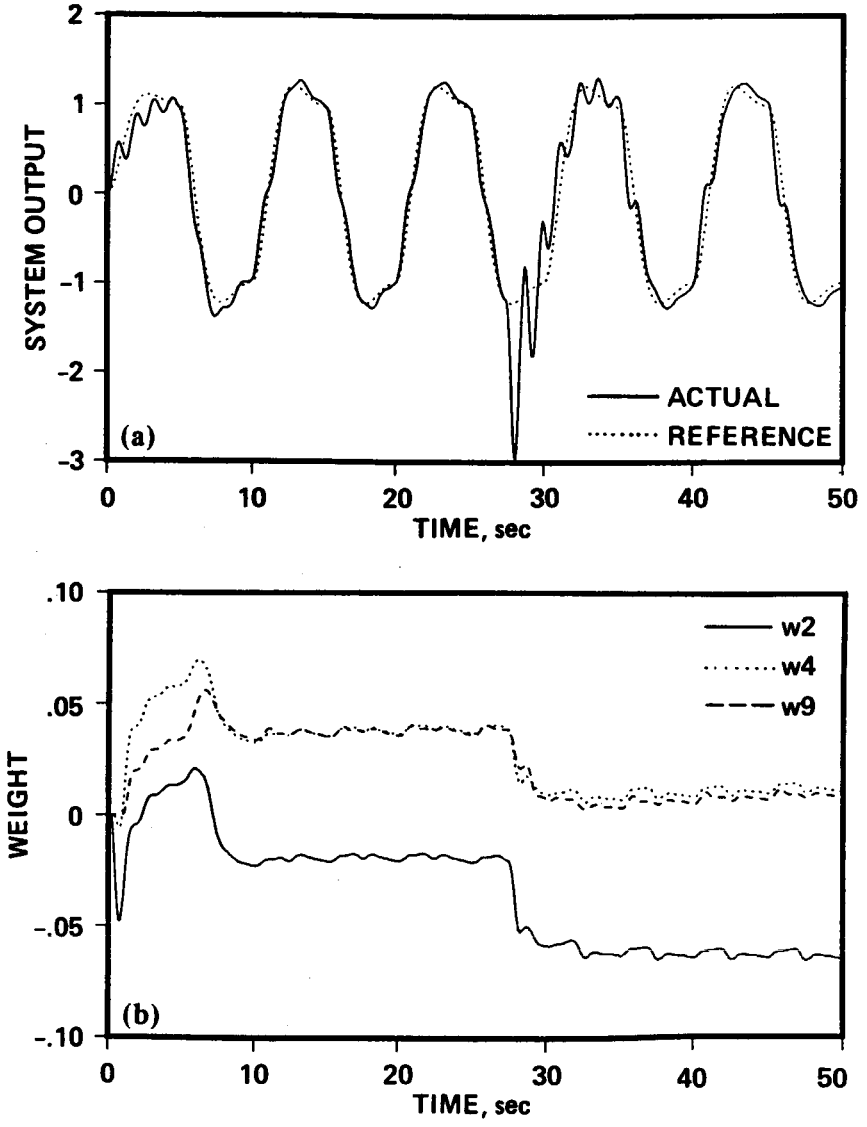

Figure 15.– Results of Run 2. (a) Actual and reference system output. (b) Time history of some filter weights.

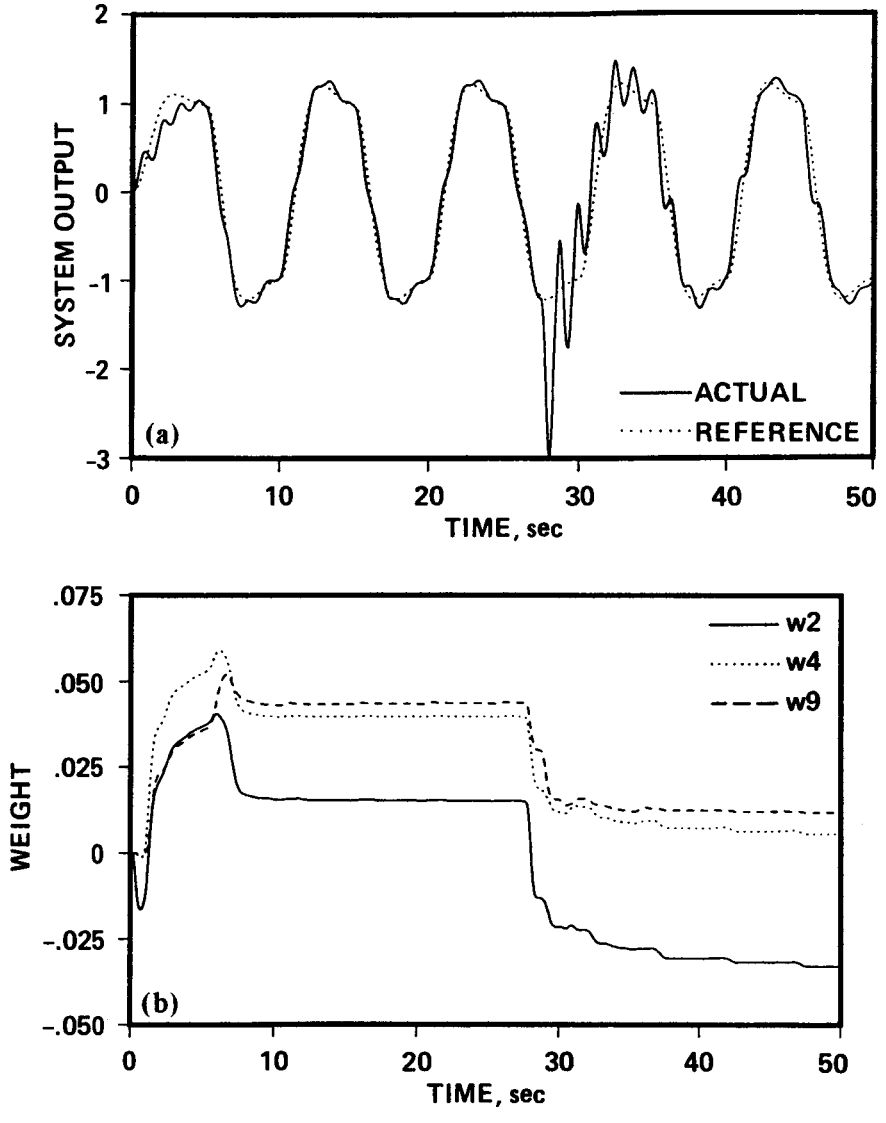

Figure 16.- Results of Run 3. (a) Actual and reference system output. (b) Time history of some filter weights.

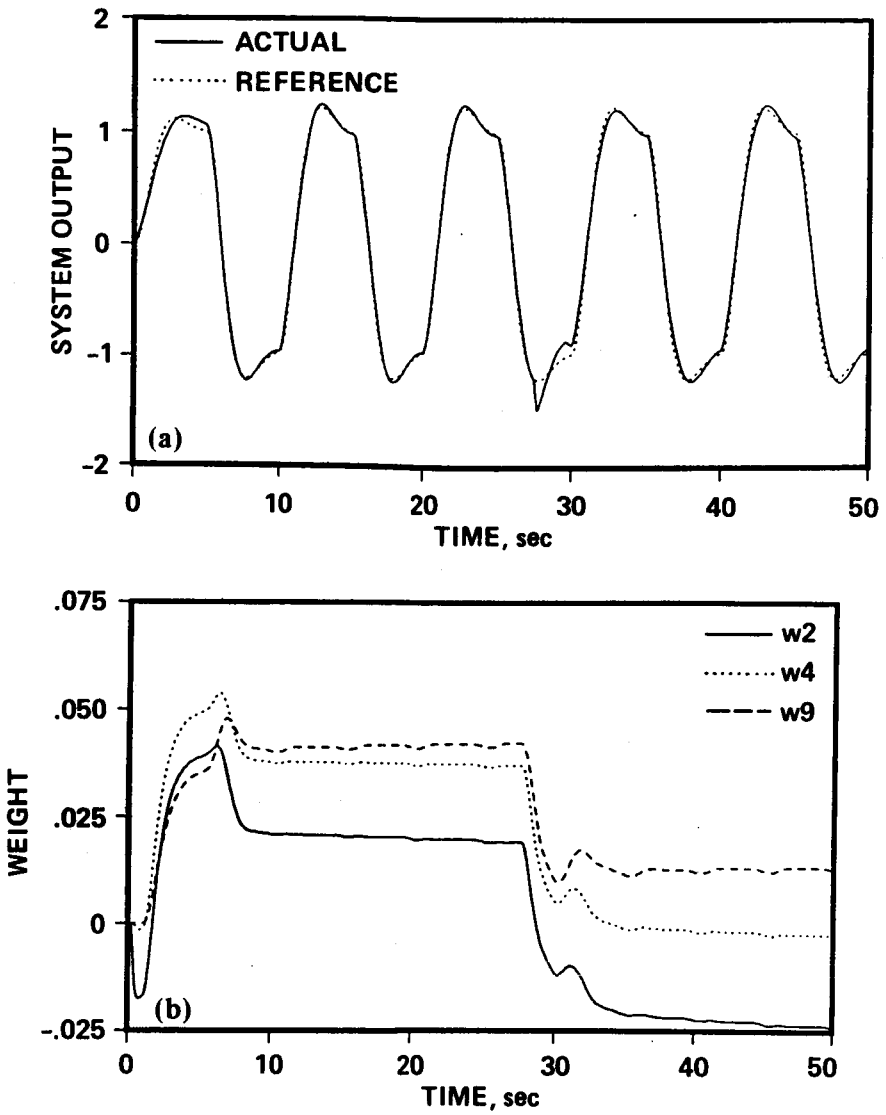

Figure 17.– Results of Run 4. (a) Actual and reference system output. (b) Time history of some filter weights.

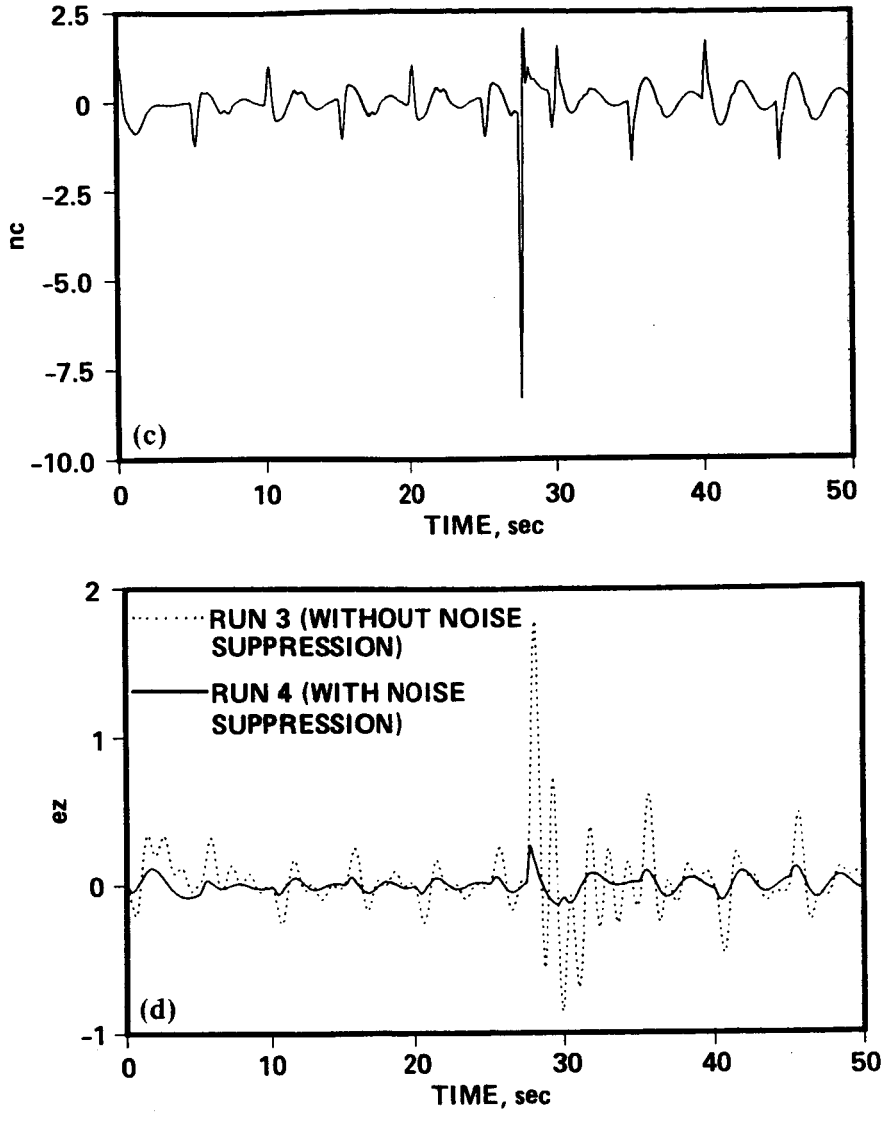

Figure 17.– Concluded. (c) Output of noise suppression loop. (d) Error in system output for runs 3 and 4.

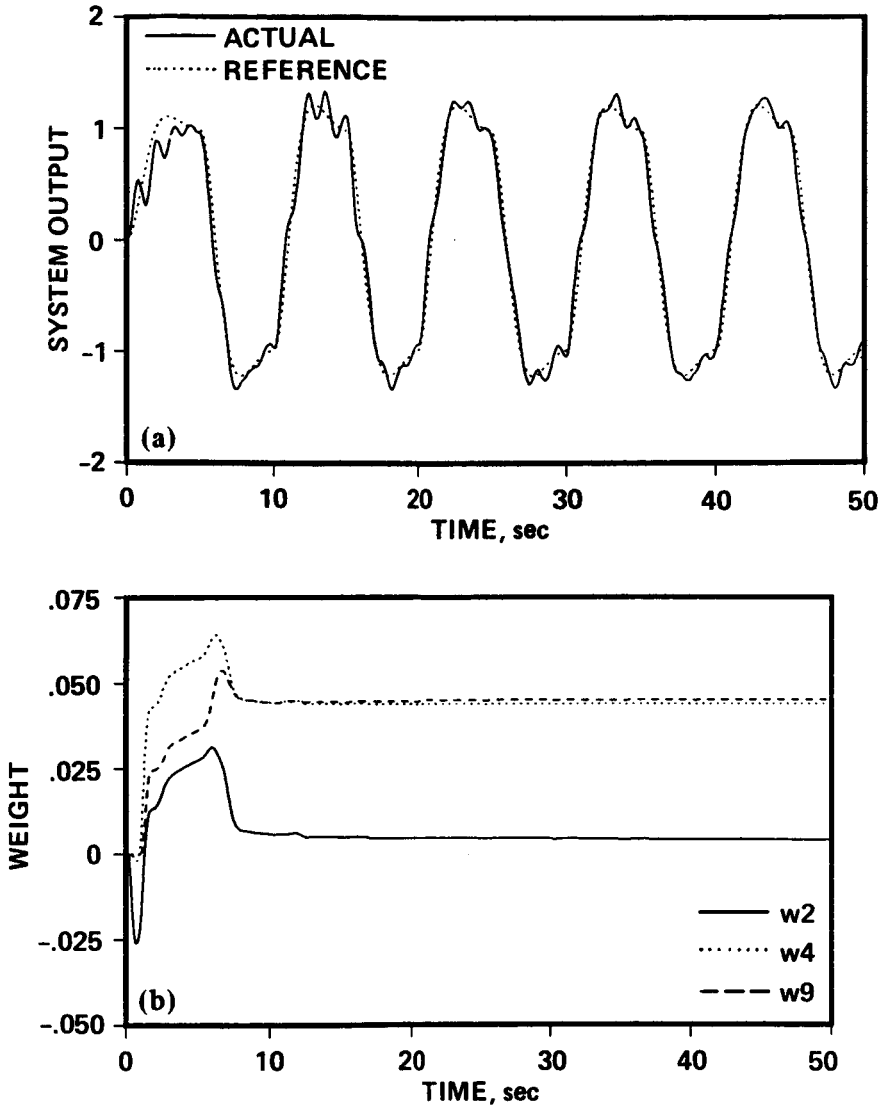

Figure 18.– Results of Run 5. (a) Actual and reference system output. (b) Time history of some filter weights.

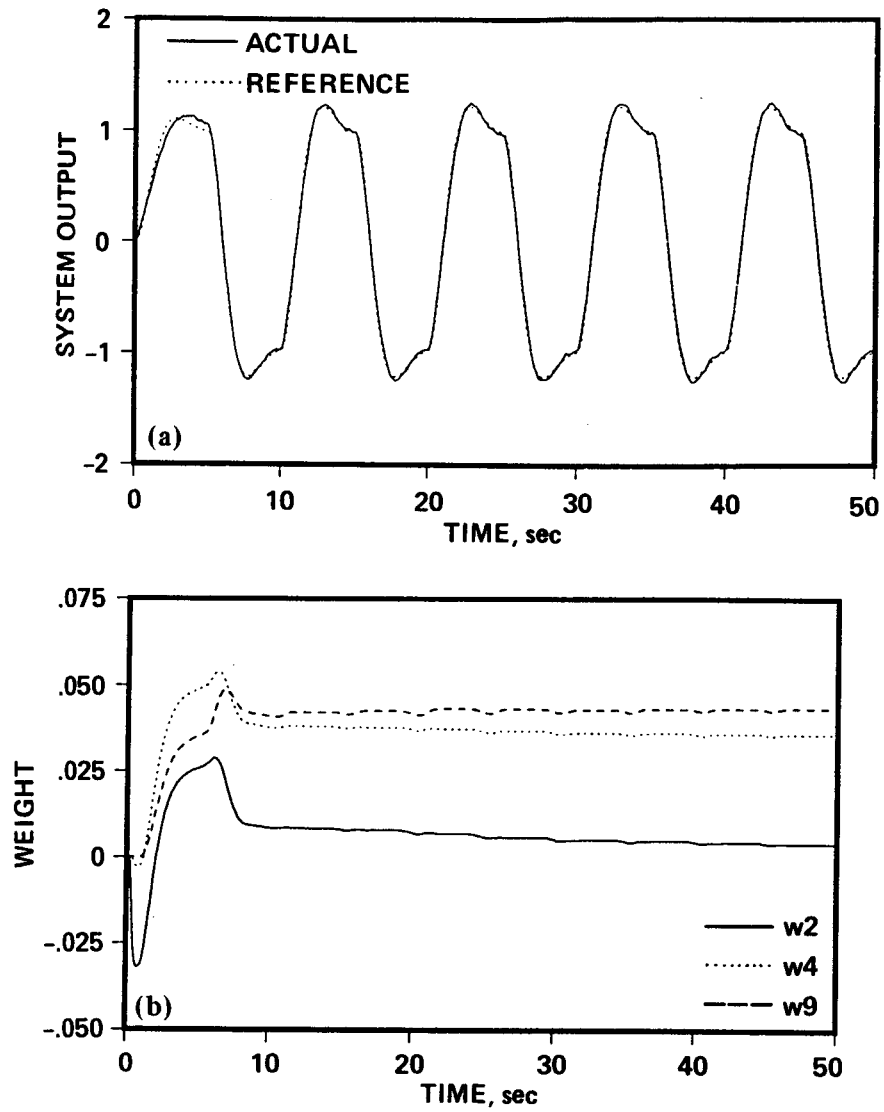

Figure 19.– Results of Run 6. (a) Actual and reference system output. (b) Time history of some filter weights.

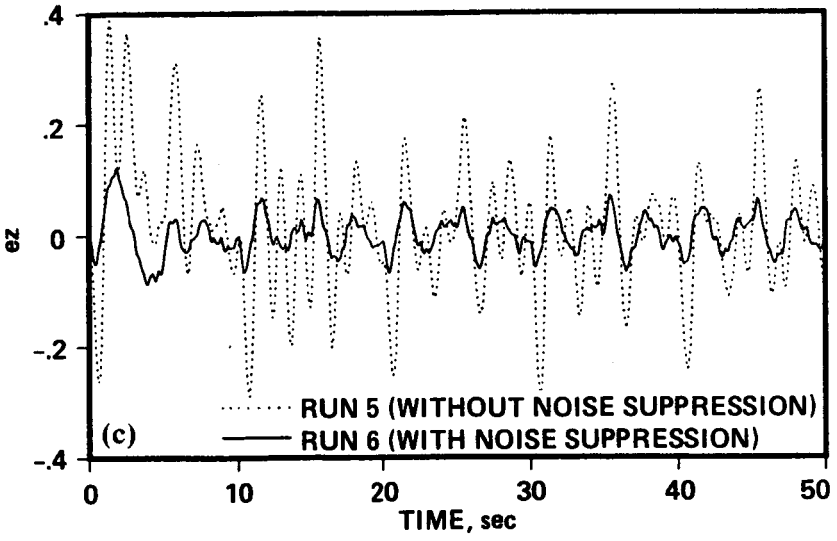

Figure 19.– Concluded. (c) Error in system output for runs 5 and 6.

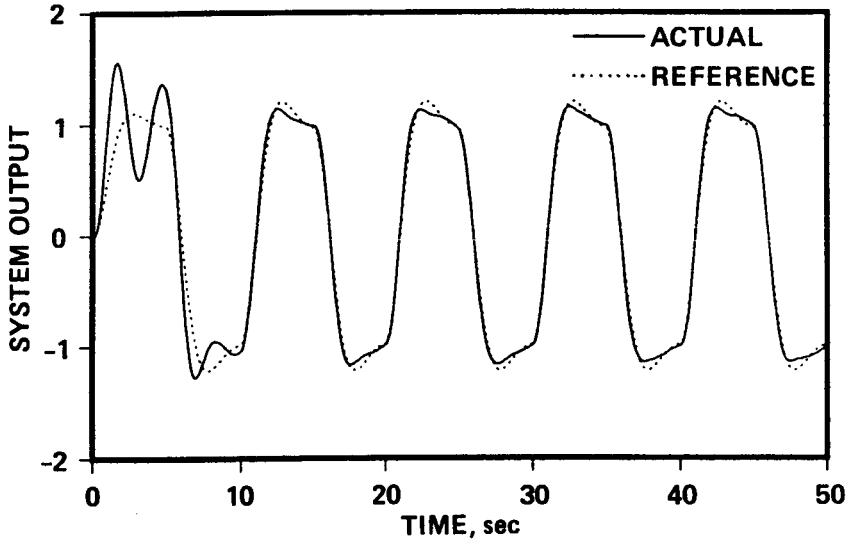

Figure 20.– Results of Run 7. Actual and reference system output.

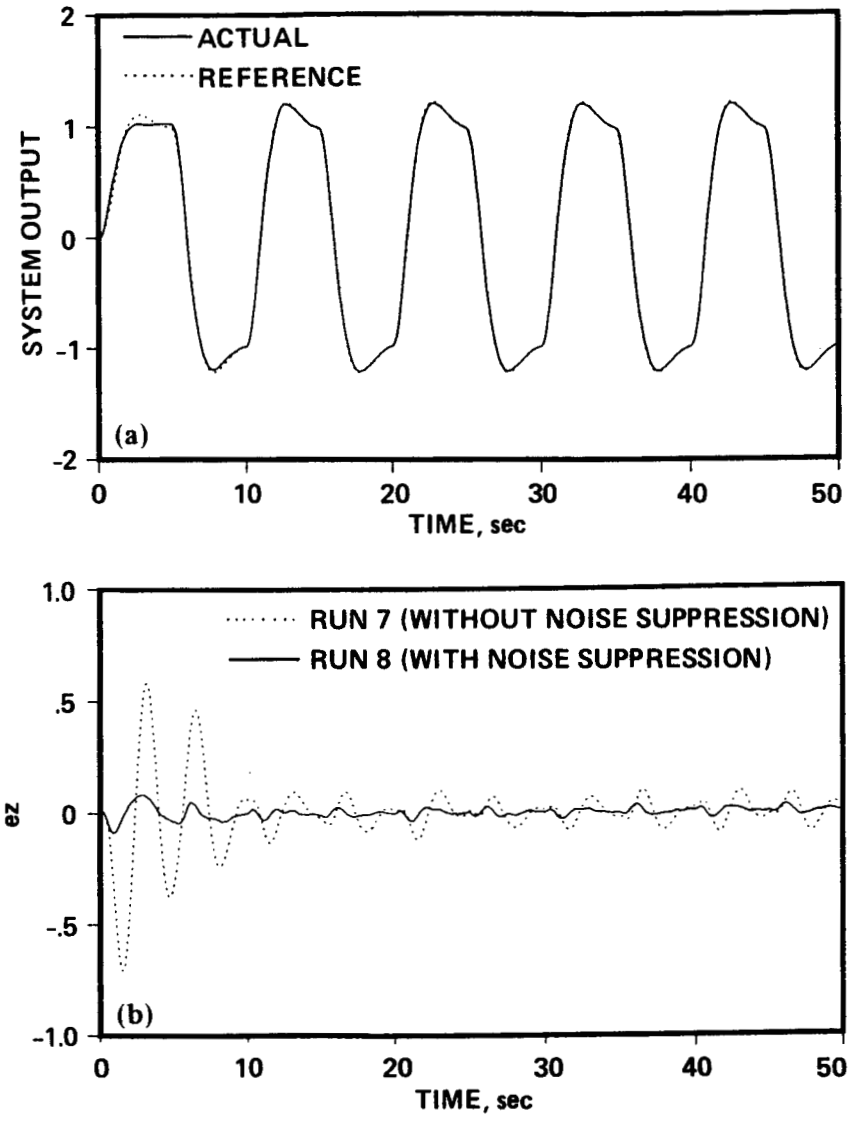

Figure 21.– Results of Run 8. (a) Actual and reference system output. (b) Error in system output for runs 7 and 8.

NASA
National Aeronautics and Space Administration

Report Documentation Page

1. Report No.	2. Government Accession No.	3. Recipient's Catalog No.
NASA TM 89453		

4. Title and Subtitle

Adaptive Control and Noise Suppression by a Variable-Gain Gradient Algorithm

5. Report Date

June 1987

6. Performing Organization Code

7. Author(s)

S. J. Merhav and R. S. Mehta

8. Performing Organization Report No.

A-87191

10. Work Unit No.

505-66-11

9. Performing Organization Name and Address

Ames Research Center
Moffett Field, CA 94035

11. Contract or Grant No.

13. Type of Report and Period Covered

Technical Memorandum

12. Sponsoring Agency Name and Address

National Aeronautics and Space Administration
Washington, DC 20546

14. Sponsoring Agency Code

15. Supplementary Notes

Point of Contact: R. S. Mehta, Ames Research Center, M/S 210-9, Moffett Field, CA 94035
(415)694-5440 or FTS 464-5440

16. Abstract

An adaptive control system based on normalized variable-gain LMS filters is investigated. The finite impulse response of the nonparametric controller is adaptively estimated using a given reference model. Specifically, the following issues are addressed: The stability of the closed loop system is analyzed and heuristically established. Next, the adaptation process is studied for piecewise constant plant parameters. It is shown that by introducing a variable-gain in the gradient algorithm, a substantial reduction in the LMS adaptation rate can be achieved. Finally, process noise at the plant output generally causes a biased estimate of the controller. By introducing a noise suppression scheme, this bias can be substantially reduced and the response of the adapted system becomes very close to that of the reference model. Extensive computer simulations validate these and demonstrate assertions that the system can rapidly adapt to random jumps in plant parameters.

17. Key Words (Suggested by Author(s))	18. Distribution Statement
Control Estimation Adaptation Stability Noise	Unclassified – Unlimited Subject Category – 66

19. Security Classif. (of this report)	20. Security Classif. (of this page)	21. No. of pages	22. Price
Unclassified	Unclassified	38	A03